VILNIUS UNIVERSITY

STATE RESEARCH INSTITUTE

CENTER FOR PHYSICAL SCIENCES AND TECHNOLOGY

Ernesta Meinorė

VARIATION OF THE PHYSICAL AND CHEMICAL PROPERTIES OF SUBMICRON ATMOSPHERIC AEROSOL PARTICLES

Doctoral dissertation

Physical sciences, Physics (02 P)

Vilnius, 2016

Dissertation was elaborated at the State Research Institute Center for Physical Sciences and Technology during the period 2011 – 2015.

Supervisor – dr. Kęstutis Kvietkus (Center for Physical Sciences and Technology, physical science, physics – 02 P).

CONTENTS

List of Abbreviations:

PM – Particulate matter

PM1 – Particulate matter in submicron range

Q-AMS – Quadrupole Aerosol Mass Spectrometer

SMPS – Scanning Mobility Particles Sizer Spectrometer

IPCC – Intergovernmental Panel on Climate Change

BBOA – Biomass Burning Organic Aerosols

CCN – Cloud Condensation Nuclei

IN – Ice Nuclei

HOA – Hydrocarbon-like Organic Aerosol

SOA – Secondary Organic Aerosols

OM – Organic matter

BC – Black carbon

EC – Elemental carbon

LV-OOA – Low-Volatility Oxygenated Organic Aerosols

SV-OOA – Semi-Volatile Oxygenated Organic Aerosols

PMF – Positive Matrix Factorization

VOCs – volatile organic compounds

TOF – Time of flight

PAH – Polycyclic Aromatic Hydrocarbons

IARC – International Agency on Cancer Research

SUMMARY

Science of atmospheric aerosol particles was commonly acknowledged as independent discipline from the mid of XIXth century, but nowadays there are still substantial uncertainties in determination of the total effect of atmospheric aerosol particles on the global climate change and the local pollution. Therefore, continuous measurements are mandatory: i) to better understand ongoing processes; ii) to predict possible consequences; iii) to maintain and implement goals of sustainable growth. This dissertation is dedicated to obtain supplementary information of physical-chemical properties of submicron range atmospheric aerosol particles (PM1) and their influence on the particle evolution.

Data of the chemical composition, concentration, size distribution of volatile and semi-volatile compounds in submicron atmospheric aerosol particles are collected at the three measurement sites: Vilnius – an urban site, Rūgšteliškis – a rural site, Preila – a coastal marine site. Analysis indicates that organics is the most abundant constituent that accounts on the average from 68.8 % to 77.1 % of the total measured volatile and semi-volatile PM1 at rural and background sites, respectively. Theoretical analysis of ammonium sulfate and ammonium nitrate contribution to the total of ammonium shows that ammonium nitrate out of all nitrates (on the average 61 ± 9 % at the Vilnius site, 61 ± 5 %, at the Rūgšteliškis site and 80 ± 3 % at the Preila site) made a greater contribution than that of ammonium sulfate out of all sulfates (37 ± 5 %, 44 ± 2 % and 36 ± 2 % for the Vilnius, Rūgšteliškis and Preila sites, respectively) to the total of ammonium. *Positive Matrix Factorization* (PMF) tool is applied to organics chemical component data for apportionment of the origin. Three factors of HOA (*Hydrocarbon-like Organic Aerosol*), BBOA (*Biomass Burning Organic Aerosols*) and SV-OOA (*Semi-Volatile Oxygenated Organic Aerosols*) are found at the Vilnius site; three factors of BBOA, SV-

OOA and LV-OOA (*Low-Volatility Oxygenated Organic Aerosols*) are indicated at the Rūgšteliškis site and two factors of LV-OOA and SV-OOA are identified at the Preila site. Constituents of organic component are recognized to be relatively more oxygenated in the SV-OOA factor, meaning that they are also more aged at the rural sites. This finding supports the presumption that long-range transport of air masses has a great impact on physical properties and overall burden of ambient aerosol particles at the remote sites.

Density of aerosol particulate matter within the particle itself is analyzed from the data collected at the urban site in Siauliai near the main street with intensive traffic. Field measurement is performed along with SMPS and Q-AMS those were deployed to collect the data. Peculiarities of obtained data were taken into consideration and therefore, corrections were applied accordingly, in order to combine data from both instruments. However, results of combined SMPS and Q-AMS data analysis stipulate that density of the particles with the diameter below 100 nm is relatively too high when compared with the density sum of all components with the diameter above 100 nm (less than 1 g cm^{-3}). Initially it was presumed that density for particles in the size range above 100 nm should exceed 1 g cm^{-3}, contrary to that of obtained results. Further analysis was conducted and it was found that deployed instruments have assigned particles according to the size erroneously; hence a correction on the diameter calculation was applied and the modeling in the density-size field was conducted. Results imply that it is erroneous to consider the same size particles to be homogeneous. Particles are emitted from different sources; therefore the particulate matter density of the same size particles may vary. It is concluded that fresh-formed particles form aggregates and their density is less than 1 g cm^{-3} in the size range less than 100 nm. Besides, the value of the median density decreases, whereas a standard deviation of the density increases with the decreasing diameter of the aerosol particles.

Data from captured volcanic pollutant episodes from 24 May until 29 May 2011 at Institute of Physics, Vilnius are evaluated in order to study the extent of particle neutralization. Two episodes are selected to analyze the extent of neutralization. The first episode is unique and enables evaluating the extent of acidic sulfates neutralization with ammonia in the atmosphere. Conducted calculations indicate that acidic sulfates on volcanic origin aerosol particles tend to be fully neutralized with atmospheric ammonia when their size is of about tenths of nanometers, whereas the larger particles have a lower extent of neutralization. Therefore, the neutralization of acidic sulfates with ammonia in volcanic origin aerosol particles can be estimated only based on the size of aerosol particles. It is also shown that ammonia is deposited on the surface area of acidic sulfates containing aerosol particles during the transfer with the air masses to the measurement site. A rough estimation of the ammonia flux onto the aerosol particle surface has been made using data of unique Episode 1; the value is estimated to be in the interval from 30 $\mu g\ m^{-2}\ h^{-1}$ to 55 $\mu g\ m^{-2}\ h^{-1}$ (in case of particle being dry, the flux would be ~74$\mu g\ m^{-2}\ h^{-1}$).

INTRODUCTION

Submicron range atmospheric aerosol particles (PM1) are of great importance due to their abundance in the ambient air and their critical abilities to influence the Earth's radiative forcing balance (global impact), burden of precipitation (regional impact) and ambient air quality (local impact).

PM1 comprises a significant fraction of the total atmospheric aerosol particles volume. Physical properties of the particles vary greatly, temporally and spatially in natural environment; therefore, it is necessary to continuously conduct measurement campaigns of ambient air in order to address the question of the present climate change globally and regionally. Accumulated knowledge from every conducted measurement allows characterizing physical and chemical properties of the particles more accurately. Furthermore, it is rather important to recognize physical properties that drive particles processes of evolution from the state of nucleation to the further growth by coagulation and formation of certain compounds.

Negative impact of PM1 on respiratory and cardiovascular health is more hazardous when compared with that of coarse particles; therefore, it is crucial to evaluate urban aerosol particles physical properties in order to address the question of urban pollutants evolution where the main source of PM1 aerosol particles is vehicles exhaust. Problem of urban pollution becomes rather important when considering that the number of vehicles is estimated to increase twice up to two billion by 2050.

In addition, the assessment of processes that could alter physical properties of volcanic origin particles during long-range transport is relevant as it is confirmed that after volcanic eruption particles can travel thousands of kilometers and influence physical and chemical properties of regional aerosol burden. Clean volcanic episodes are unique and rare in long-range transport air

masses, hence captured data are significant and their analysis contributes to a better understanding of particles evolution processes during advection.

The aim of the study

The aim of the study is to characterize volatile and semi-volatile submicron range atmospheric aerosol particles along with developing measurement and analysis methods and indicating physical and chemical properties that influence particles evolution processes.

Tasks:

1. To characterize the abundance of volatile and semi-volatile atmospheric PM1 aerosol particles chemical components, to determine their dependence on prevailed long-range air masses and to define the origin of organics component at urban and background sites in Lithuania.
2. To examine the contribution of ammonium sulfate and ammonium nitrate to that of the total ammonium in submicron range aerosol particles.
3. To assess PM1 organic matter density of aerosol particles with the diameter less than 100 nm under ambient conditions of intensive traffic emission at an urban site.
4. To evaluate the extent of atmospheric neutralization of submicron volcanic origin aerosol particles containing acidic sulfates with atmospheric ammonia in long range transport air masses.

Scientific novelty

1. A method that enables accurately estimating the distribution of organic matter density in aerosol particles with the diameter below 100 nm is developed.

2. The extent of atmospheric neutralization of acidic sulfates containing particles with atmospheric ammonia in the submicron range is estimated.

Scientific actuality

1. Executed quantitative analysis of ammonium nitrate and ammonium sulfate contribution to the total of ammonium supplements the knowledge regarding particles formation processes.
2. The developed method of density assessment of organics within the aerosol particles with the diameter below 100 nm can be implemented in the air pollution models.
3. The analysis of the neutralization extent of volcanic origin acidic sulfates containing particles with atmospheric ammonia augments the knowledge about particles evolution and its dependence on physical properties. Derived results can be implemented using models for assessment of precipitation acidity.

Statements to defend

1. Organics comprise a significant fraction of the total measured volatile and semi-volatile PM1 mass in submicron atmospheric aerosol particles during mild season at the urban and background sites in Lithuania.
2. Concentration variance of sulfate and nitrate enables determining ammoniun nitrate out of all nitrates and ammonium sulfate out of all sulfates contribution to that of total ammonium.
3. Fresh–formed particles from precursors of transport emission, with the diameter below 100 nm, combine agglomerates or aggregates and have a different organic matter density distribution. Organic matter density

within aerosol particles in the size range below 100 nm is lower than 1 g cm^{-3}.

4. The extent of neutralization of acidic sulfate with atmospheric ammonia in volcanic origin aerosol particles can be estimated only based on the size of aerosol particles and those below 100 nm tend to be fully neutralized.

List of publications

Publications published in periodic scientific journals

1) **Meinorė, E.,** Šakalys, J., Kvietkus, K., 2014, Chemical composition, concentration and source apportionment of atmospheric submicron aerosol particles at urban and background sites, Lith. J. Phys., 54, 4, 244-255.
2) Šakalys, J., **Meinorė, E.,** Valiulis, D., Dudoitis, V., Kvietkus, K., Ulevičius, V., 2015, Density assesment method of chemical components in urban submicron aerosol particles, Lith. J. Phys., 55, 2, 142-152.
3) Šakalys, J., **Meinorė, E.,** Kvietkus, K., 2016, Neutralization of acidic sulfates with ammonia in volcanic origin aerosol particles, Lith. J. Phys., 56, 1, 42-48.

Thesis at international and national conferences

1) Kvietkus, K., Šakalys, J., **Meinorė, E.,** Didžbalis J., Diurnal variation of submicron aerosol particles and fluctuation on their chemical components concentration in the vicinity of Vilnius city, 40-oji Lietuvos nacionalinė fizikų konferencija, Vilnius, 2013 m.
2) Kvietkus, K., Šakalys, J., **Meinorė, E.,** Didžbalis, J., Chemical composition, concentration, size distribution and diurnal variation of atmospheric submicron aerosol particles at the background and urban

sites in Lithuania, The 2013 European Aerosol Conference, Czech Republic, Prague, 2013.

3) Šakalys, J., Kvietkus, K., **Meinorė, E.,** Neutralization of sulfates with ammonia in volcanic origin aerosol particles (*Vulkaninės kilmės sulfatų neutralizacija amoniaku aerozolio dalelėse*), 41-oji Lietuvos nacionalinė fizikų konferencija, Vilnius, 2015.
4) Šakalys, J., **Meinorė, E.,** Valiulis, D., Dudoitis, V., Kvietkus, K., Ulevičius, V., Density assessment method of chemical components in urban submicron aerosol particles, The 2015 European Aerosol Conference, Italy, Milan, 2015.

1 LITERATURE OVERVIEW

Pollution of atmospheric air is one of the crucial challenges faced by the society, although the existence of the issue is dated back to 3rd - 1st century BC. Student of Aristotle admitted: "*smell of burning coal was disagreeable and troublesome*". Philosopher Seneka documented about the intolerable air of Rome: "*As soon as I had escaped the heavy air of Rome and the stench of its smoky chimneys, which when stirred poured forth whatever pestilent vapours and soot they held enclosed, I felt a change in my disposition".* Atmosphere is enriched with the myriad of natural or/and anthropogenic impurities called atmospheric aerosol particles or particulate matter (PM). Atmospheric aerosol particles are mainly of a natural origin being a part of the Earth's self-sustainable thermal balance system. However, since the start of industrial revolution in the late 18th to mid 20th centuries the anthropogenic pollution of ambient air has reached unbearable extent especially in the major cities, where industrialization process was intensive. Combustion of low quality coal in the factories and households significantly contributed to the pollution of the ambient air. Major cities had experienced several severe onsets of the smog (a fog that contains particles from emission of industrial activities, particularly soot particles and sulphur dioxide - SO_2) followed by the increased mortality rate and deterioration of the respiratory system health. From tens to hundreds deaths were recorded during the severe smog onsets and thousands negative impacts on respiratory health were reported. For example: Meuse Valley fog in Belgium (1930), factory emission of fluorine gasses (Roholm, 1937) was related to 60 deaths and has caused several thousands cases of respiratory tract illness; St. Louis Smog in U.S. (1939) referred as "Black Tuesday"; hydrogen fluoride and sulfur dioxide have composed The Donora smog in U.S. (1948) that resulted in 20 deaths (50 more relevant deaths were recorded within a month after the onset) and nearly 7 000 were affected; The Great Smog of London (1952) resulted in 12 000 deaths (Bell et al., 2008) and nearly 100 000

were affected by illness; Harbin smog in China (2013) is related with an increase of respiratory health issues by one fifth. Severe cases of air pollution have led authorities to take legislative attempts under regulatory approaches underlying commitment to reduce emission of pollutants (i.e. Clean Air Acts, Kyoto protocol, Paris agreement and etc.). The environment friendly activity under the approach of sustainable growth was declared to be a priority. One of the sustainable growth key steps is to reduce the impact of human activity on the change of the mean global temperature. The emission of natural particles (i.e. emission from volcanoes) cannot be managed, even though it is crucial to fully understand the interaction and ongoing processes within the atmospheric constituents. Atmospheric aerosol particles both of anthropogenic and those of natural origin are attributed to have an impact on the change of global temperature, yet the overall mechanism of their influence is not fully understood.

This dissertation chapter covers a literature overview on atmospheric aerosol particles. Particular attention is paid to distribution of the particulate matter density in aerosol particles and neutralization processes of the volcanic origin particles in the long-range air masses.

1.1 Atmospheric aerosol particles

Atmospheric aerosol particles or also referred as particulate matter (PM) is a disperse system of solid-state or/and liquid particles suspended in a liquid and/or gaseous medium in an ambient air. There are two main kinds of atmospheric aerosol particles in respect of their origin: particles of natural origin and those of anthropogenic origin that are attributed to be the result of human activity. The other substantial partition describes whether a particle is primary or secondary. Primary particles are directly emitted from the sources into atmosphere whereas the secondary particles are formed during the gas-to-

particle conversion processes **(**homogenous or heterogeneous nucleation and condensation processes of gaseous precursors). Both primary and secondary particles can be either of natural or of anthropogenic origin. Main sources of naturally occurring primary aerosol particles are volcanoes, soil erosion, sea spray, mineral dust, desert dust, biological debris, humic matter, microbial particles (microorganisms, bacteria, algae, pollen, viruses). Major part of anthropogenic emission consists of fossil fuel combustion, industrial activities and transport exhaust. Tropospheric aerosol particles mostly consist of ammonium, nitrate sodium, chloride, sulfate, crustal elements, water, volatile organic compounds (VOCs), organic matter and trace metals. It is estimated that aerosol particles of natural origin comprise from 2200 Tg/yr to 24000 Tg/yr whereas those of anthropogenic origin from 320 Tg/yr to 640 Tg/yr (Table 1-1; Hinds, 2012). Such a wide range of uncertainty for natural aerosol particles is mostly due to unpredictable emissions of volcanoes and sea spray.

Table 1-1. Sources and estimates of global emissions of atmospheric aerosol particles (Hinds, 2012)**.**

	Range Tg/yr [10^6 metric tons/yr]	**Best Estimate** Tg/yr [10^6 metric tons/yr]
SOURCE		
Natural		
Soil dust	1000-3000	1500
Sea Salt	1000-10000	1300
Botanical debris	26-80	50
Volcanic dust	4-10000	30
Forest fires	3-150	20
Gas–to–particle conversion	100-260	180
Photochemical	40-200	60
Total of natural sources	2200-24000	3100
Anthropogenic		
Direct emissions	50-160	120
Gas–to–particle conversion	260-460	330
Photochemical	5-25	10
Total of anthropogenic sources	320-640	460

Aerosol particles greatly vary in shape, size, and chemical composition hence meaning that they are also spatially and temporally highly variable. Particles can be spherical or non-spherical; they can form conglomerates or aggregates (Fig. 1-1). Their lifetime in the atmosphere alters from a few hours to a few weeks and depends on their physico-chemical characteristics (Raes et al., 2002; Williams et al., 2002).

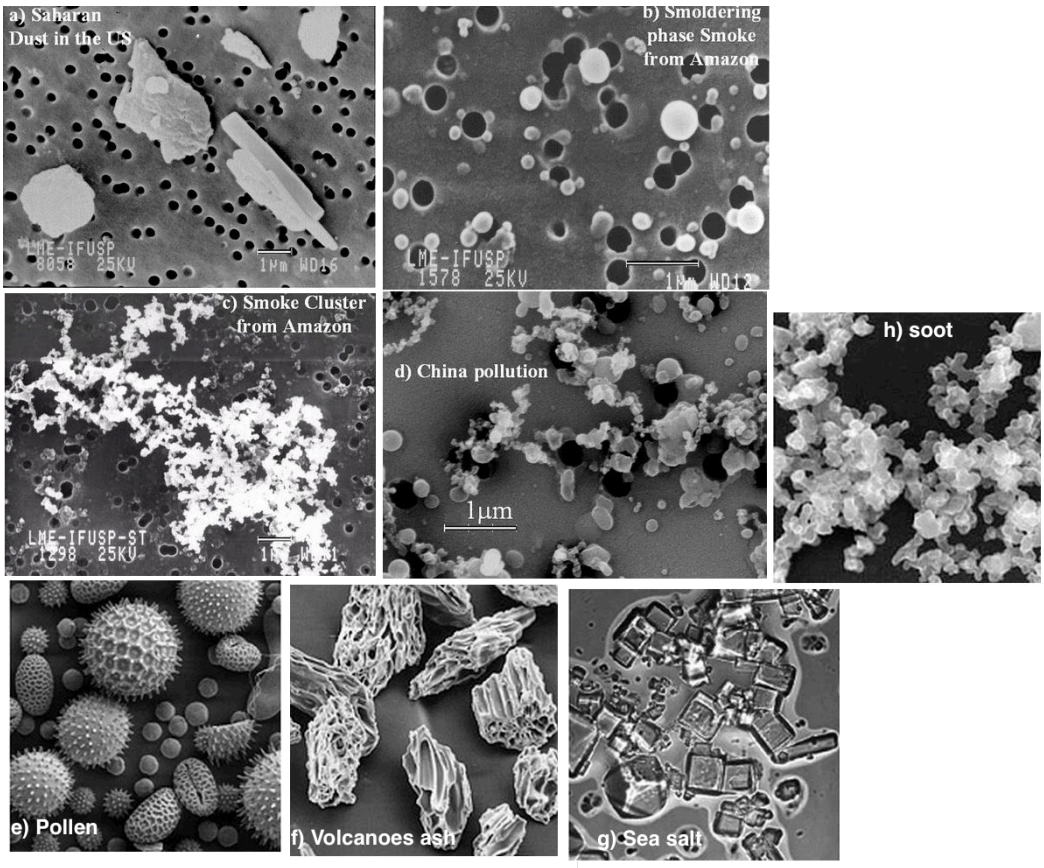

Fig. 1-1. Variability in size and shape of aerosol particles (adopted from http://earthobservatory.nasa.gov/Features/Aerosols/).

The size of the atmospheric aerosol particles usually varies from a few nanometers to 100 μm. Bigger particles are not considered as atmospheric aerosol particles. Particles are assigned to certain modes in respect of their formation and pathways of washouts from the atmosphere, usually referred as

atmospheric sinks. Two fundamental modes of atmospheric aerosol particles are fine (< 1 μm) and coarse (>1 μm). Fine mode is divided into nucleation mode, also known as ultrafine mode (< 0.01 μm), Aitken mode (0.01–0.1 μm) and accumulation mode (0.1–1 μm) (Fig. 1-2). If we compare – human hair is 60 μm.

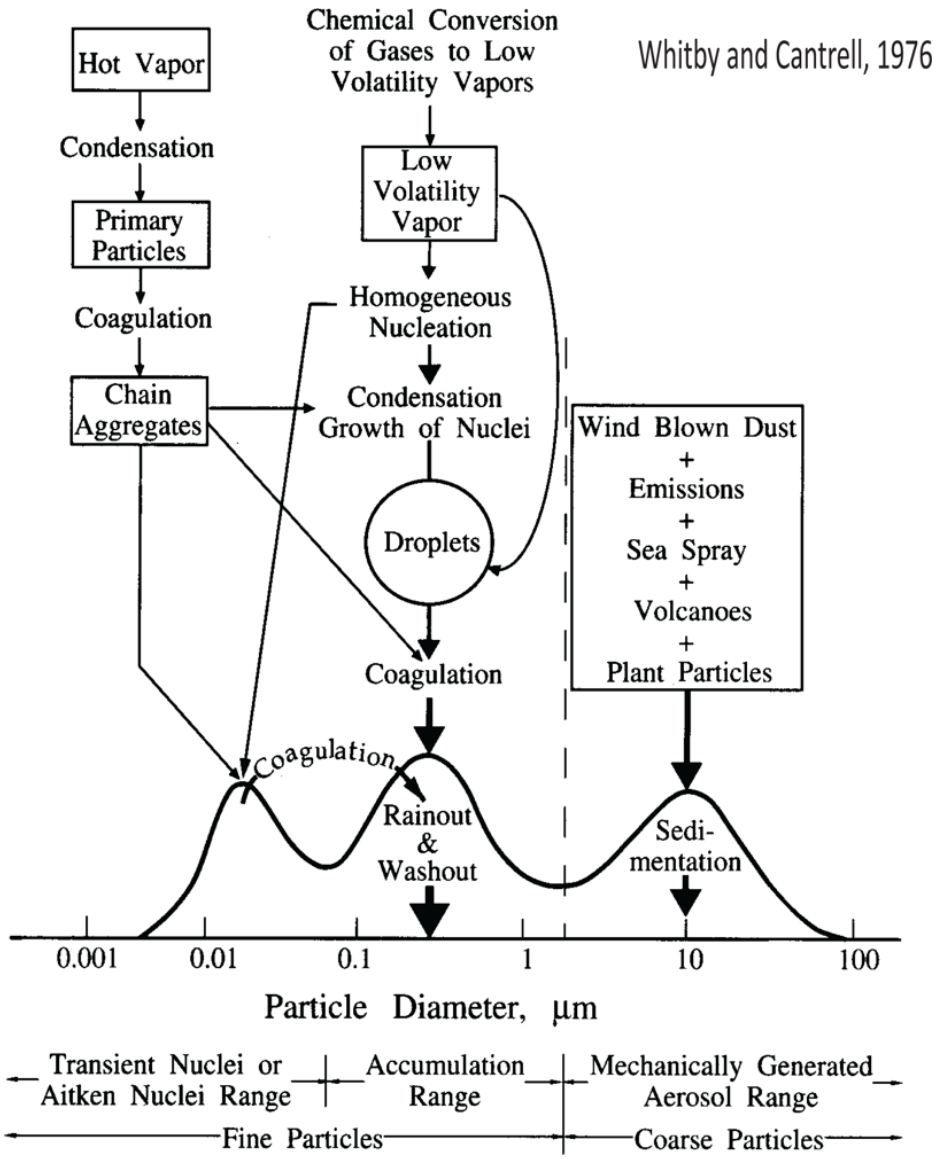

Fig. 1-2. Partition of aerosol particles in respect of the modes and mechanisms of particles wash outs from the atmosphere (Whitby K. T., Cantrell B. K., 1976).

Particles from the atmosphere can be removed either through dry deposition (when particles are deposited onto Earth's surface) or wet deposition (when Cloud Condensation Nuclei (CCN) is formed followed by the removal in the form of precipitation). Mechanism of particles being washed out

from the atmosphere depends on their size. It is estimated that coarse particles are deposited relatively faster than the fine particles with the velocity of 3×10^{-3} m s^{-1} and 3×10^{-5} m s^{-1}, respectively (Seinfeld and Pandis, 2006). Particles with the diameter larger than 10 µm settle slowly by gravitational forces; however particles with diameter of over 150 µm are already not concerned as aerosol particles because of relatively fast sedimentation rate (Seinfeld and Pandis, 2006). The particles with the diameter between 0.1 µm and 1 µm (most commonly sulfates and nitrates) are likely to have the sedimentation velocity of less than 1.0×10^{-3} m s^{-1} (Table 1-2; Harrison, 1999). The most likely route for their removal from the atmosphere is through CCN, Ice Nuclei (IN), and rain droplet formation mechanism (Fig. 1-2).

Table 1-2. Sedimentation velocity in respect of particles size when density of the particle is 2 g cm^{-3} (Harrison, 1999).

Diameter (µm)	Sedimentation velocity (m s^{-1})
<1	$<1.0 \times 10^{-3}$
5	1.5×10^{-3}
10	6.1×10^{-3}
20	2.4×10^{-2}
50	4.6×10^{-1}
150	8.0×10^{-1}
>150	> 1

The size of the particle is characterized by the particle diameter; however, most of the particles are non-spherical, hence the term of equivalent diameter is considered to be more appropriate to describe the particle. In general it describes the particle sedimentation rate as if it were spherical. The derived equivalent diameter depends on measurement techniques and employed instruments, i.e., D_{va} – the vacuum aerodynamic diameter is obtained if Q-AMS (Quadrupole Aerosol Mass Spectrometer) is used, D_m – the electrical mobility diameter if SMPS (Scanning Mobility Particles Sizer Spectrometer)

system is used. Most commonly used term is the aerodynamic diameter. The aerodynamic diameter is an equivalent diameter that describes the sedimentation velocity of a non-spherical particle that has the same sedimentation velocity as the spherical particle with the same diameter in the gaseous environment. The shape factor is included in the diameter calculation in case of non-spherical particles. Calculation of the aerodynamic diameter is as follows:

$$D_a = D_g k \sqrt{\frac{\rho_p}{\rho_0}}, \tag{1.1}$$

D_g – the geometric diameter, k – the shape factor (for spherical particles $k = 1$), ρ_p – the density of the particle, ρ_0 – the density of water (1 g cm^{-3}).

1.2 Primary and secondary aerosol particles

Natural primary aerosol particles mainly originate from volcanoes (mostly sulfur dioxide), sea spray (sea salt and dimethylsulfide oxidation products), desert/soil dust, wildfire smoke and vegetation processes (mostly terpenes and isoprene), whereas anthropogenic emission sources are mainly vehicles, industry and combustion processes in urban areas. Secondary aerosol particles are usually formed from gaseous precursors either of the natural or anthropogenic origin. Interaction between the natural and anthropogenic aerosol particles, and secondary aerosol particles formed due to this interaction are still the field of an active research. Secondary organic aerosol (SOA) particles are usually formed during homogeneous nucleation, condensation and heterogeneous reactions of gas-phase oxidation products from a natural (biogenic) as well as anthropogenic volatile and semi-volatile organic compounds (Zaveri et al., 2012), whereas secondary non-organic aerosol particles are formed from sulfate and ammonium nitrate compounds (Seinfeld and Pandis, 2006). Studies have shown that components of primary aerosol

particles (especially semi-volatile compounds) can be desorbed into gas-phase compounds before the secondary aerosol is formed, meaning that compounds undergo oxidation before secondary particle is formed (Robinson et al., 2007). These findings lead to the conclusion that the low-volatility gas phase precursors, including long chain n-alkanes, polycyclic aromatic hydrocarbons (PAHs) and large olefins, are a potentially large source of SOA (Dall'Osto and Harrison, 2012). Burden of secondary non-organic aerosol particles is mostly enhanced during the following reactions in the atmosphere:

$$2NO_2 + O_2 + 2H_2O \rightarrow 2HNO_{3(gas)},$$

$$2SO_2 + O_2 + 2H_2O \rightarrow 2H_2SO_{4\ (liquid)},$$

$$HNO_{3\ (gas)} + NH_{3\ (gas)} \rightarrow NH_4NO_{3\ (solid)},$$

$$H_2SO_{4\ (liquid)} + 2NH_{3\ (gas)} \rightarrow (NH_4)_2SO_{4\ (solid)}.$$

However, other secondary aerosol particle components are not yet recognized (Goldstein et al., 2008), and the conditions leading to the formation of secondary aerosol particles are unclear (Hallquist et al., 2009).

1.3 Atmospheric aerosol particles effect on the average global temperature and human health

The qualitative negative effect of aerosol particles on human health, on the quality of air and the particle ability to influence the mean global temperature are widely acknowledged (Chio and Liao, 2008; Dockery and Pope, 1994; IPCC, 2013, 2007; Ovadnevaite et al., 2006; Pope and Dockery, 2006; Solomon et al., 2007; Straif et al., 2013). Aerosol particles are an integral part of the natural Earth's biosphere. However, since naturally

ubiquitous aerosol particle burden is enhanced by that of anthropogenic origin a natural equilibrium of particles is imbalanced.

The effect on human health will be briefly described therein after. Impact of atmospheric aerosol particles on the mean global temperature can be derived in terms of radiative forcing that is measured in Wm^{-2} units. Radiative forcing is defined as the difference between scattered and absorbed solar radiation. Thirty percent of annual solar radiation reaching the Earth's atmosphere is backscattered to space, 77 % of it is backscattered due to atmospheric aerosol particles and only 23 % by the Earth's surface (Trenberth et al., 2009). Aerosol particles act both by directly and indirectly scattering and absorbing solar radiation: directly absorbing or/and scattering solar radiation back to space by aerosol particles themselves and indirectly by forming CCN or/and IN (Lohmann and Feichter, 2004). Intergovernmental Panel on Climate Change key finding with a very high level of confidence confirms that the interaction between atmospheric aerosol particles and clouds acts in an opposite way from that of the green house gases (Fig. 1-3) (IPCC, 2013).

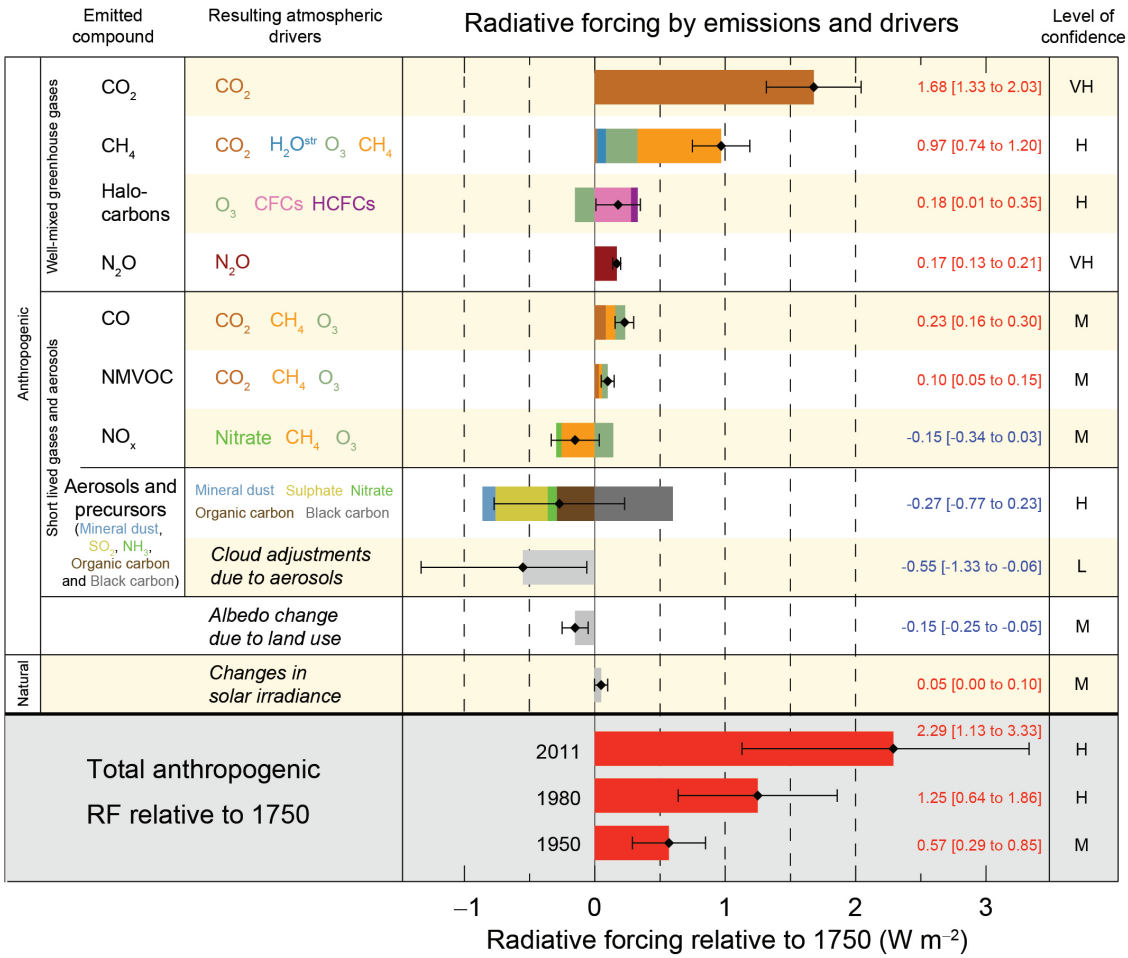

Fig. 1-3. Radiative forcing estimates in 2011 relative to 1750 and aggregated uncertainties for the main drivers of climate change (IPCC, 2013).

Net effect of atmospheric aerosol particles on global mean temperature is negative (cooling) and as a result the Earth's albedo is increased. Contrary, direct absorption of solar radiation by aerosol particles has a warming effect and leads to CCN evaporation. Certain regions might be suffering from drought as a result of CCN evaporation followed by the suppressed ratio of precipitation. Whether solar radiation will be absorbed or scattered depends on the aerosol particles size distribution and chemical composition. It is clearly understood that the green house gases together with atmospheric aerosol particles are the drivers of the temperature change, but however there is still a substantial portion of uncertainty on estimations of atmospheric aerosol particle impact on radiative forcing. The net effect of aerosol particles on

radiative forcing is still a subject of discussions. However, the present knowledge allows us to calculate that the overall effect of the aerosol particles and the green house gases combined is positive (meaning green house gases warming effect wins versus aerosol particles cooling effect) and is mainly caused by the increase of atmospheric CO_2 emission since 1750 (Fig. 1-3).

The increasing concentration of atmospheric aerosol particles results in increased cardiovascular and respiratory tract illness ratio (Dominici et al., 2006; Ovadnevaite et al., 2006). It is observed that the concentration of 10 – 20 µg m^{-3} or higher is related to the increase of the population illness rate. It is especially observable in cardiovascular and lung disease cases. The particles with the diameter less than 10 µm are inhalable. Once inhaled ultrafine particles can penetrate to alveoli, whereas particles of a larger size can settle in trachea (Fig. 1-4) or can be filtered by mucus membranes. The smaller the particle, the greater the hazard it can cause.

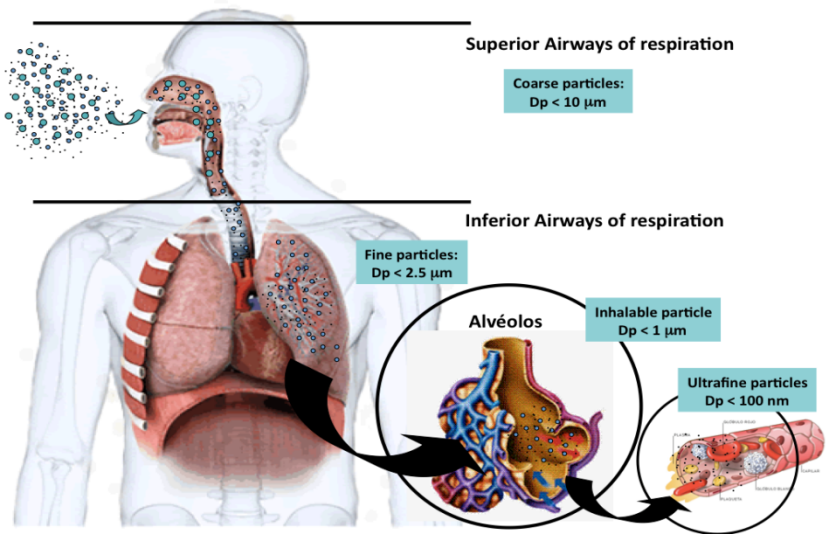

Fig. 1-4. Aerosol particles deposition in the human airways in respect of particle size (Guarieiro and Guarieiro, 2013).

If the coarse particles are deposited onto the area of superior airways of respiration tract they can be easily removed by natural human processes within

a matter of hours once a certain amount of the particle concentration is accumulated. Ultrafine particles, however, are inhaled into interior airways of respiration and penetrate to the alveoli. Finally, chemical compounds that comprise particles are distributed over the body through the blood circulation system. Further more, harmful compounds can be transported into lymph nodes and cause various illness. It is usually nearly impossible to detect and clarify the cause of illness in such kind of cases, unless it is known that a human was exposed to severe ambient air pollution.

1.4 Aerosol particles size distribution

Atmospheric aerosol size resolved distribution is usually described in terms of normal distribution (Fig. 1-5).

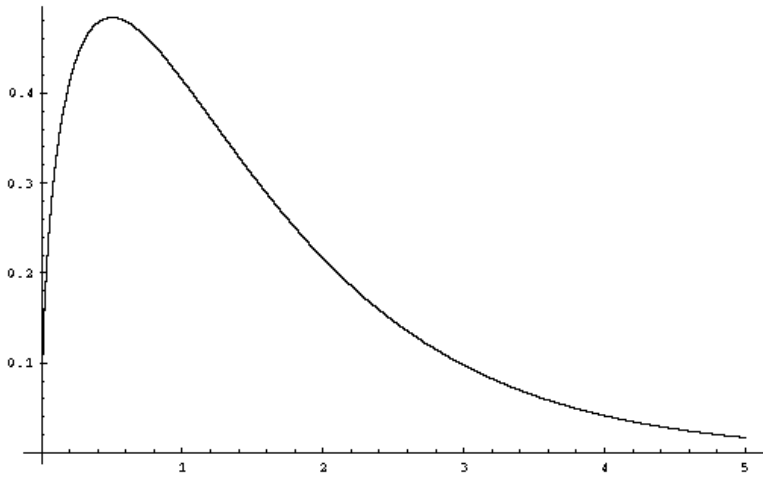

Fig. 1-5. Maxwell – Boltzmann normal distribution.

Normal distribution is often encountered and accommodated in daily practice. Normally, the atmospheric aerosol particles size distribution is depicted by the logarithmic aerodynamic diameter value on abscise axis (rarely natural logarithmic values of aerodynamic diameter are used). Maxwell distribution

could be retrieved in the ideal case of the particles size-distribution. The reason for data depiction on a logarithmic scale is rather trivial. It is done for the convenience purposes only. Distribution data are easily comparable within outcome of different experiments once presented in this way.

The median value (1.2) and the standard deviation (1.3) are logarithmic normal components that well describe the lognormal particle size distribution.

$$\log d_g = \frac{\sum_i n_i \log d_i}{\sum_i n_i} \tag{1.2}$$

$$\log \sigma_g = \left[\frac{\sum_i n_i (\log d_g - \log d_i)}{\sum_i n_i - 1} \right]^{\frac{1}{2}} \tag{1.3}$$

Where d_g – the mean diameter, σ_g – a standard deviation, n_i – the number of particles in the interval i, d_i – the mean diameter of interval i.

Usually lognormal distribution is applied to every single mode during data analysis:

$$\frac{\mathrm{d}m}{\mathrm{dlg}D} = \frac{\mathrm{d}m_1}{\mathrm{dlg}D_1} + \frac{\mathrm{d}m_2}{\mathrm{dlg}D_2} + \frac{\mathrm{d}m_3}{\mathrm{dlg}D_3} \tag{1.4}$$

Where m – the total mass, D – the resultant diameter, D_1 – the diameter of mode 1, m_1 – the mass of mode 1, D_2 – the diameter of mode 2, m_2 – the mass of mode 2, D_3 – the diameter of mode 3, m_3 – the mass of mode 3.

Or it can be written as:

$$\frac{\mathrm{d}m}{\mathrm{d}\lg D} = \frac{M_1}{\lg \sigma_1 \cdot \sqrt{2\pi}} \mathrm{e}^{-\frac{(\lg D_{vid.} - \lg D_1)^2}{2 \lg \sigma_1^2}} + \frac{M_2}{\lg \sigma_2 \cdot \sqrt{2\pi}} \mathrm{e}^{-\frac{(\lg D_{vid.} - \lg D_2)^2}{2 \lg \sigma_2^2}} + etc... \tag{1.5}$$

Where $M_{1,2,...}$ – the mass of certain modes, $D_{1,2,...}$ – the diameter of certain modes.

Most commonly nucleation and accumulation modes of $d_g = 0.034$ μm, $\sigma_g = 1.8$ and $d_g = 0.090$ μm, $\sigma_g = 2.0$ values are observed in Lithuania.

1.5 Chemical composition of submicron aerosol particles in Lithuania

Anthropogenic origin aerosol particles from industry, transport and agricultural activities are the main source of pollution in Lithuania. Nevertheless, the natural origin aerosol particles such as dust of volcanoes are advected with the long-range transport air masses and sea spray aerosol particles are noticeable at the seashore line of Lithuania.

Organics comprise from 20 % to 90 % of the entire aerosol volume of the PM1 (Jimenez et al., 2009; Kanakidou et al., 2005; Zhang et al., 2007). Several studies in Vilnius have also shown that fraction of organics is dominant, with the mass concentration ranging between 74.1 % and 82.7 % of all volatile and semi-volatile non-refractory PM1 compounds, whereas the nitrate concentration is between 4.6 % and 7.7 % (Kvietkus et al., 2011). Very similar results were obtained at the rural coastal/marine site of Preila (station of atmospheric pollution research) where organics accounted for about 60 % of all measured PM1 upon advection of North-Atlantic air masses in the study of Rimselyte et al. (2007) and that of 80 % in the study of Garbariene et al. (2012). Three factors were identified by Positive Matrix Factorization from organic data at a coastal/marine site of Preila during the campaign in 2006: LV-OOA – aged oxygenated low-volatility organic aerosol, SV-OOA less oxygenated semi-volatile organic aerosol and BGOA – biogenic organic aerosol (with no distinction between marine and continental origin) (Garbariene et al., 2012).

1.6 Density of particulate matter within aerosol particles

The density of aerosol particles is highly variable in time due to the ongoing processes or/and chemical reactions in the atmosphere and within the particle itself. Distribution of the density is also a variable that depends on the myriad of factors; i.e., high mass concentration could have a lower number concentration and vice versa. Examination of the ultrafine particle density is of high importance and is more likely to be considered when discussing the adverse effect of the urban airborne particles on the human health (Li et al., 1996). Density of the matter determines processes within the particles themselves and with ambient particles in an urban environment. Density is one of the crucial characteristics in the models of pollutants transmission. Change of the density distribution is most likely to be prompt in the urban environment where exhaust emission comprises a significant fraction of the anthropogenic pollution burden.

Generally, exhaust emitted and freshly formed particles fall into the ultrafine size range and constitute 90 % of the total particles volume in an urban environment (Kannosto et al., 2008). A relative drop in a mean diameter due to the increased consumption of biodiesel is reported in (Lin et al., 2007). Moreover, as reported in Chien et al. (2009), the trend of particles being shifted towards ultrafine and nanometer size ranges results in an increase of the certain size aerosol particle density as the blending of biodiesel increases in urban areas.

According to Kannosto et al. (2008) measurements of particle density can provide valuable information about the attribution of particles to the certain modes (i.e. separation into Aitken and accumulation mode) in accordance with the origin of the particles. On the other hand, chemical composition is one of the essential factors for the particle formation and further growth (Kulmala et al., 2006), in any case the density of a chemical compound within the particle has a significant implication. Therefore, the distribution of density of the

chemical component within the particle could be acknowledged as the most important characteristic. It determines optical, chemical and mechanical properties of aerosol particles, and therefore the sedimentation rate by altering the aerodynamic diameter of the particles. The density of distribution of a certain chemical compound is a complex, time-dependent characteristic which is influenced by the aerosol particle chemical composition, chemical reactions between the particle components themselves and within the atmosphere. For example, sulfuric acid is attributed to the species responsible for the particle formation event at urban sites in several studies (Brus et al., 2011). However, recent studies imply that different species of organics are responsible for the particle growth in natural environment (Ristovski et al., 2010). Vapors are recognized to be responsible for the change of the particle growth, but the role of other abundant species remains unrecognized (Ehn et al., 2006). Moreover, the distribution of density of a chemical compound for a single aerosol particle should be taken into consideration due to the conclusions presented by the International Agency for Research on Cancer (IARC), where outdoor air pollution is classified as carcinogenic to humans (Straif et al., 2013).

In general, the very first results of particle density observations were reported in Hanel and Thudium (1977) where low efficiency and time-consuming sample techniques of pycnometer were used. The density of the particles varies greatly during the city campaigns reported in several studies. Assuming that all particles are spherical the density in the range from 1.54 g cm^{-3} to 1.77 g cm^{-3} was shown in the study of McMurry et al. (2002); the range from 1.0 g cm^{-3} to 1.5 g cm^{-3} was reported by Spencer et al. (2007); the effective particle density of 1.62 ± 0.38 g cm^{-3} for $PM_{1.8}$ and 1.67 ± 0.37 g cm^{-3} for PM_{10} was reported in Hu et al. (2012). It should be stressed that effective densities are comparable only if the values are calculated in the same manner (Hu et al., 2012; Slowik et al., 2004). It is interesting to note that the rural mode resolved particle density reported in Kannosto et al. (2008) is 0.5 – 1.5 g cm^{-3}, 0.97 g cm^{-3} and 1.5 g cm^{-3} for nucleation, Aitken and accumulation

mode, respectively. The density of 1.36 g cm^{-3} was shown in Malloy et al. (2009) where Scanning Mobility Particle Sizer (SMPS) – Aerosol Mass Spectrometer (AMS) setup was used. It should be pointed out that when SMPS – AMS setup is used the density and the shape of the particle are crucial characteristics for derivation of the mass concentration. Nevertheless, the particles with the same mobility are likely to have distinct masses (McMurry et al., 2002), meaning they have the different density, that is important for determination of the relationship between the electric mobility and the aerodynamic diameter (Morawska et al., 1999; Schmid et al., 2007). The combined effect of the particle electric mobility and the shape as the effective particle density determines its mechanics (DeCarlo and Slowik, 2004; Malloy et al., 2009).

1.7 Volcanic origin aerosol particles

During the volcanic eruption a variety of gases are emitted into the atmosphere. The most abundant species are vapor of water (H_2O), carbon dioxide (CO_2) and sulfur dioxide (SO_2). Other species are also released with a smaller amount: hydrogen sulfide (H_2S), hydrogen chloride (HCl), carbon monoxide (CO), hydrogen (H_2), helium (He) and hydrogen fluoride (HF) (Table 1-3, Symonds et al., 1994). After the eruption volcanic particulate and gaseous emissions, e.g. sulfuric dioxide, instantly interact with atmospheric water and eventually form acidic aerosol particles (i.e. once sulfur dioxide is oxidized with OH the sulfuric acid is produced (Solomon et al., 2007)).

Table 1-3. Composition of volcanic emission (a few examples) (Symonds et al., 1994).

Volcano	Kilauea Summit	Erta` Ale	Momotombo
Tectonic Style	Hot Spot	Divergent Plate	Convergent Plate
Temperature	1170°C	1130°C	820°C
H_2O	37.1	77.2	97.1
CO_2	48.9	11.3	1.44
SO_2	11.8	8.34	0.50
H_2	0.49	1.39	0.70
CO	1.51	0.44	0.01
H_2S	0.04	0.68	0.23
HCl	0.08	0.42	2.89
HF	_	_	0.26

Pollutants from volcanic eruption favor secondary acidic aerosol formation after a plume of sulfur dioxide is exhaled to the atmosphere during eruption. Volcanoes are one of the largest sulfur dioxide sources in the North Atlantic region releasing about 0.9 Tg yr^{-1} of sulfuric dioxide (Halmer et al., 2002). Particulate and gaseous volcanic emission can cause air traffic disarray (e.g. Eyjafjallajökull eruption in 2010, Grimsvötn eruption in 2011) and adverse effect on the environment and human well-being (hazard to aircrafts, reduction of visibility). The major impact on air traffic is observed within 24 hours at up to 1000 km distance from the eruption site (Guffanti et al., 2009), but volcanic material trace is observed even for up to 100 hours a few thousand kilometers away from the eruption site (Adame et al., 2015). Perturbation of local gases and particle budget due to volcanic emission is observed farther than 3000 km (Adame et al., 2015; Kerminen et al., 2011; Kvietkus et al., 2013; Ovadnevaite et al., 2009). Characterization and identification of volcanic

origin particles are still an issue due to their ability to be mixed with pollutants present in the lower and upper atmosphere.

1.7.1 Neutralization of volcanic origin particles

Acidic sulfate particles of volcanic origin are neutralized with ambient ammonia in the atmosphere. The major sources of ammonia in the atmosphere are agricultural activities including livestock and fertilization of soil with ammonium containing compounds, although ammonia is also captured over the oceans. Other sources of ammonia are: soil and ocean evaporation, industry processes and emission from transport (Behera et al., 2013). Consequently, whether a fully neutralized or highly acidic sulfate particle is captured at the measurement site depends on the available amount of ammonia in the atmosphere during the process of advection. The main agent of neutralization for acidic sulfate particles is ammonia. The excess of present ammonia takes part in neutralization of organic acidic particles in the atmosphere (Mensah et al., 2012), furthermore, it is also found that the presence of organic gases reduces the rate of ammonia uptake and the ambient acidic particles may longer remain in acidic state than previously expected (Liggio et al., 2011). However, ammonia concentrations are higher in the troposphere rather than in the boundary layer hence, the extent of instant neutralization also depends on the height of volcano eruption plume (Fisher et al., 2011).

In a broader context the extent of neutralization of acidic sulfuric particles is important for estimating radiative forcing which comprises a few parameters, two of which should be stressed here: ice nucleation and scattering of solar radiation which generally results in atmospheric cooling (Baustian et al., 2010; Martin et al., 2004; Quinn et al., 2008). Ice nucleation is favored by the products of partial neutralization of acidic sulfate with ammonia: solid ammonium sulfate $(NH_4)_2SO_4$ (ammonium to sulfate molar ratio 2),

ammonium bisulfate NH_4HSO_4 (ammonium to sulfate molar ratio 1.5), letovicite $(NH_4)_3H(SO_4)_2$ (ammonium to sulfate molar ratio 1). The model presented in Fisher et al. (2011) suggests that usually neutralization of aerosols that originate in Europe is f=0.75 ($f = [NH_4^+]/[2SO_4^{2-}] + [NO_3^+]$ in molar units, nitrate is almost neglected due to its low concentration) at an elevation of 2 km. In the study of Biskos et al. (2009) it is demonstrated that partial neutralization depends on the particle size and is more significant than any other nano-size effect for hydroscopic growth of dry particles as small as 5.5 nm at the relative humidity of 80 %. Furthermore, Skrabalova et al. (2014) confirmed that at a fixed relative humidity the hygroscopic growth deteriorates as the particle diameter decreases owing to a greater extent of neutralization. Interesting observation reported by Kulmala et al. (2004) suggests that particles with the diameter of 10 nm contain only ~20–30 % of sulfate, therefore it gives a strong support for the conclusion that the extent of neutralization strongly depends on the particle size. In addition, the same study of Kulmala et al. (2004) confirmed that the extent of neutralization of sulfate plays a key role in nucleation mechanisms in the atmosphere. In the study of Mcmurry et al. (1983) it was observed that ammonia (gas) – sulfuric acid (aerosol) chemical reaction rate during neutralization was two-fold lower for particles with the 100 nm diameter and was equal to 0.18±0.03, whereas that for 58 nm diameter particles was equal to 0.40±0.10. Other studies were also consistent with the conclusion that reaction rates decrease along with the increase of neutralization in low relative humidity.

1.8 Chapter conclusion

Science of atmospheric aerosol particles as a stand-alone discipline was accepted in the late 19th century. The origin of the particles, the distribution of aerosol size, the chemical composition, optical, spatial and temporal properties were essential characteristics in order to address the question of the aerosol particle impact on our environment ever since. Findings and conclusions varied greatly over the decades along with available probing instrumentation. Experimental instruments and evaluation techniques of obtained data have been improved greatly in terms of accuracy and probing size so that accumulated knowledge and findings are more likely to be profoundly confident and precise at these times. It is shown that science of atmospheric aerosol particles is of great interest especially today as the society is being laid in front of the challenge of the global climate change. The role of natural primary or/and secondary and anthropogenic primary or/and secondary atmospheric aerosol particles is acknowledged to be one of the main drivers. Many schemes and processes within the particles themselves and interaction with atmospheric constituents as well as their formation from ambient precursors are already known. However, there is still a certain portion of uncertainty within the main characteristics that can complement the description of ambient aerosol particles. Therefore it is one of the important parts of the puzzle to determine physical and chemical properties that could possibly alter the particle behavior in ambient environment.

Previous studies have analyzed coastal/marine site in terms of source apportionment in Lithuania, but there are fewer studies from the urban and the rural areas from the data obtained with Q-AMS. Furthermore, there was no analysis of the contribution of ammonium nitrate out of all nitrates compounds and ammonium sulfate out of all sulfates compounds to the total of ammonium from Q-AMS data.

Density of the matter within the aerosol particle is considered to be one of the crucial variables for models of particle aging and pollutant transmission. Density of the matter can change dramatically over a short period of time due to traffic emissions in urban areas. Therefore, a method for PM1 organic constituent density assessment is developed from obtained Q-AMS and SMPS data evaluation.

Studies suggest that volcanic eruption can cause perturbation on local aerosol particle properties farther than a few thousands kilometers from the eruption site. Nevertheless, episodes of pure volcanic pollutants distant from the source are rare, thus data of advected volcanic pollutants physical properties are largely lacking. Therefore, captured relatively clean volcanic pollutants episode allowed analyzing the extent of natural neutralization of submicron acidic sulfates with atmospheric ammonia in volcanic origin aerosol particles advected with long-range transport air masses further than 3000 km.

2 METHODOLOGY

This chapter provides information on measurement sites, instrumentation and PMF method. Description of each measurement site is presented followed by the explanation of performed measurement. Detailed description on instrumentation used is also provided and the basic idea of the statistical evaluation method PMF (Positive Matrix Factorization) is briefly described.

2.1 Measurement sites

Data of the chemical composition, concentration, and source apportionment of PM1 were collected at three measurement sites: Vilnius – an urban site, Rūgšteliškis – a rural site, Preila – a coastal site (Fig. 2-1, black squares indicated). Density of aerosol particulate matter within the particle was analyzed from the data collected during the measurement campaign between 15 March and 27 March in 2012 in one of the main streets of Šiauliai town (Fig. 2-1, red square indicated). To study the extent of particle neutralization, data from captured volcanic pollutant episodes from 24 May until 29 May 2011 at Institute of Physics, Vilnius were evaluated (Fig. 2-1 Vilnius site).

Measurement sites and campaigns for characterization of PM1. The urban sampling site was located at Institute of Physics near the city of Vilnius (54°38′36′′N; 25°10′57′′E), an industrial center with a population of over 520.000 and a residential area of 400 km^2. Two power stations near the sampling site, one to the north-west and the other to the east, could be mentioned concerning the influence on local aerosol particle parameters, while in the south and west, there are no important sources of pollution. The rural Rūgšteliškis sampling site was located in a national park in Aukštaitija. Boreal

and Scots pine trees forest surrounds sampling site (55º27´48´´N, 26º03´60´´E). The average air temperature is about 5.8°C, the highest point of the area is about 188.6 m ASL and there are no considerable point pollution sources. Data from the coastal sampling site was collected at the Preila Environmental Pollution Research Station on the coast of the Baltic Sea (55º22´34´´N, 21º01´52´´E, 5 m a. s. l.). Pollution research station is located on the Curonian Spit where marine weather conditions dominate. The range of air temperature in winter and in summer is rather small when compared to its standard continental differences. The Curonian Spit has relatively mild winters and cool summers than those on the continent, however strong winds dominate there all the year round. The closest possible pollution sources are the village of Preila (2.5 km away to the east), but due to low population (~ 300 inhabitants) the anthropogenic emission effect is negligible and not considerable, Nida (~1200 inhabitants) 10 km to the south and the city of Klaipeda (~160 000 inhabitants) at a 40 km distance to the north. The Rūgšteliškis and Preila sites are considered to be background sites with no considerable point pollution sources around. Data were collected during three measurement campaigns in 2011: from March 23 to June 5 at Vilnius sampling site, from June 17 to July 1 at the Rūgšteliškis site and from July 3 to August 24 at the Preila site.

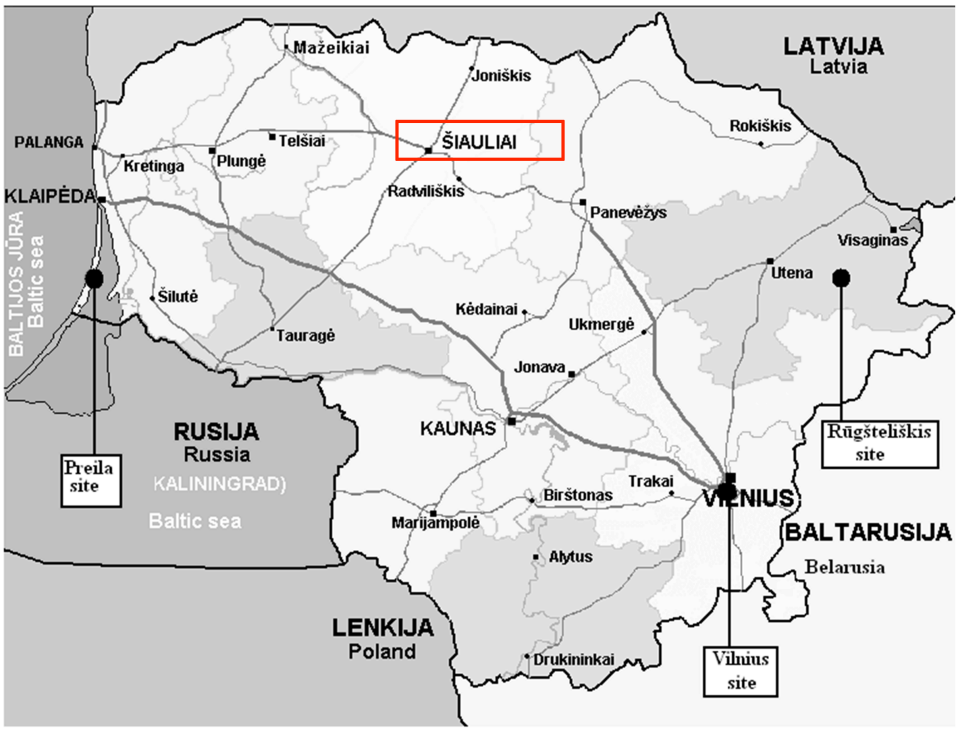

Fig. 2-1. Measurement sites.

Campaign for PM1 density analysis. Density of aerosol particulate matter within the particle was analyzed from the data collected during measurement between 15 March and 27 March in 2012 in one of the main streets of Šiauliai town (Fig. 2-1, red square indicated). Population in Šiauliai is over 100 thousand, and the town is situated in the north of Lithuania. The instruments (Q-AMS and SMPS) for measurement campaign were deployed at the air quality monitoring station ($55^0$56´16,11´´N and $23^0$18´29,68´´E). The monitoring station is under considerable influence of traffic emissions due to the location in a main street near the shopping mall.

Campaign for the extent of neutralization analysis. To study the extent of particle neutralization, data from captured volcanic pollutant episodes from 24 May until 29 May 2011 at the Institute of Physics, Vilnius were evaluated (Fig. 2-1). The episodes of the increased concentration were detected after the air masses from the Grimsvötn volcano eruption on 21 May 2011 had reached the measurement site.

2.2 Instruments and methods

2.2.1 Quadrupole Aerosol Mass Spectrometer

The Quadrupole Aerosol Mass Spectromer (Q-AMS) is designed by Aerodyne Research, Inc. It was used to obtain quantitative real-time size resolved distribution and chemical composition of ambient volatile and semi-volatile non-refractory (it is referred to the particles that vaporize on the time scale of < 100 μs at 600 °C) PM1 components. Q-AMS was deployed for all the campaigns presented in this paper. The instrument provides the real-time chemical composition and mass size distribution of non-refractory chemical components (sulfate (SO_4^{2-}), ammonium (NH_4^+), chloride (Cl^-), nitrate (NO_3^-) and organics) present in ambient atmospheric aerosol particles at a temporal resolution of 5 min. Q-AMS determines certain compounds with regard to the m/z ratio (Table 2-1, Canagaratna et al., 2007).

Table 2-1. Basic fragments of molecular ions for identification of chemical compounds present in aerosol particles (Canagaratna et al., 2007).

Compound	Ion fragments	Mass to charge ratio (m/z)
Water (H_2O)	**H_2O^+**, HO^+, O^+	**18**, 17, 16
Ammonia (NH_3)	NH_3^+, **NH_2^+**, NH^+	17, **16**, 15
Nitrates (NO_3)	HNO_3^+, **NO_2^+**, NO^+	63, **46**, 30
Sulfates (H_2SO_4)	$H_2SO_4^+$, HSO_3^+, SO_3^+, **SO_2^+**, **SO^+**	98, 81, 80, **64, 48**
Hydrocarbons (C_nH_m)	$C_nH_m^+$	27, 29, 41, 43, 55, **57,** 69, 71, …
Organic compounds (oxidated) ($C_nH_mO_y$)	H_2O^+, CO^+, **CO_2^+**, $H_3C_2O^+$, HCO_2^+, $C_nH_m^+$	18, 28, **44**, 43, 45

Q-AMS does not efficiently detect low-volatility materials such as black carbon, *NaCl,* crustal oxides and certain metals. It provides information on volatile and semi-volatile compounds in aerosol particles with limited single-particle information. The instrument consists of three main parts: the particle beam inlet chamber, the particle sizing chamber and the detection chamber. Sections of the instrument combine vacuum and mass spectrometric techniques with aerosol sampling techniques (Fig. 2-2).

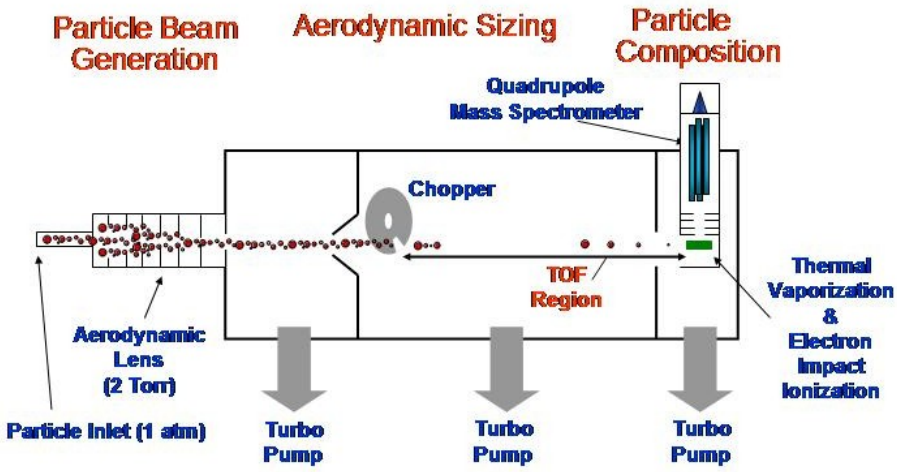

Fig. 2-2. Schematic picture of Q-AMS, Aerodyne Research Inc., Massachusetts (adopted from ww.mpic.de).

Particles enter the sampling chamber through the inlet that restricts the flow with 100 µm critical orifice at the pressure of 267 Pa. After entering the sampling chamber, aerosol particles are focused into a collimated beam of 1 µm while passing through an aerodynamic lens system (Liu et al., 1995). The aerodynamic lens system consists of 6 apertures (Fig. 2-3). The core of the sampling method superior to the capillaries and nozzles is that the aerodynamic lenses are able to focus particles of various sizes into the collimate beam without charging the particles.

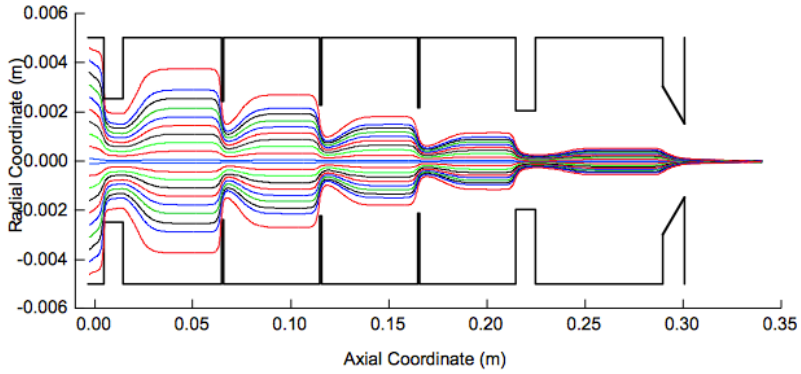

Fig. 2-3. Calculated particle trajectory for unit density and 100 nm diameter spheres through the aerodynamic lens system.

Performance of the lens is the most effective if the size of the particle is in the range between 40 nm and 500 nm (Fig. 2-4). Particles smaller than 40 nm in diameter are not focused due to the lack of inertia, hence the majority of them follow the gas streamline, and the ones larger than 500 nm in diameter are not focused due to excessive inertia. For example, particles of NH_4NO_3 (dry ammonium nitrate particles of 300 nm are usually used for the instrument calibration) with the diameter between 70 nm and that of 500 nm reach the detector with the efficiency of 100 % whereas for smaller than 70 nm in diameter and larger than 500 nm the detection efficiency declines greatly. Brownian motion and lift forces determine the possible minimum width of the collimated beam (Liu et al., 1995).

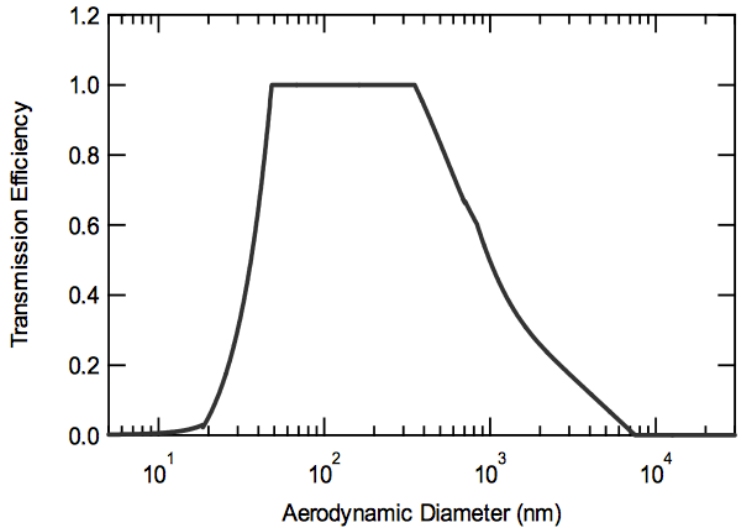

Fig. 2-4. Particle transmission efficiency as a function of particle size (Jayne et al., 2000).

Once the beam of particles exits the lens system particles are accelerated in supersonic expansion that is induced by the different pressure between sampling and sizing chambers. Ambient gas is removed by differential pumping. Therefore, particles gain different terminal velocity in respect to their size and mass. The smaller the particle size, the higher the terminal velocity. After entering the size-sampling chamber the beam of focused particles is intercepted by the rotating chopper wheel (5 cm in diameter). The chopper wheel has two radial splits located 180 ° apart. There are three modes that the chopper wheel could be positioned at: i) particle beam is open, the chopper is positioned that all particles can get through the radial split; ii) particle beam is chopped - partially blocking the beam, chopper rotates and allows passing only through the radial split; iii) particle beam is blocked – no particles can get throughout the chopper, background is measured. Throughput when the partially opened chopper position is set is only from 2 % to 3.5 % of the total operating time; hence it allows separating particles into 25 categories of mass. Photodiodes are used to determine the position of the chopper wheel slits and the start of each cycle. Time of Flight (TOF) between the chopper and the

detector where particles are flash vaporized within the timespan of a few μs describes the velocity of the particle; thus, the aerodynamic diameter could be determined. Once particles reach the surface of tungsten usually heated up to ~600 ºC, non-refractory particles are flash vaporized under the pressure of ~10^{-8} Torr. The vapor plume is ionized by means of the 70 eV electron impact ionization source. The resultant positive ions are focused into the quadrupole, which acts as a mass-to-charge (*m/z; z=q/e*) filter. Ions with a certain *m/z* ratio emerging at the exit of quadrupole are recognized and directed to the electron multiplier for a fast multiplication of the order of 10^6.

It needs to be noted, that Q-AMS measures the vacuum aerodynamic diameter since TOF is measured in free-molecular regime flow, contrary to the classically obtained aerodynamic diameter that is obtained in the conditions of continuum regime flow. Relation between the aerodynamic and vacuum aerodynamic diameter can be expressed as follows:

$$D_{va} = \frac{\rho_p}{\rho_0} \cdot \frac{D_v}{\chi_v} \text{ (Jimenez, 2003)} \qquad (2.1)$$

where D_{va} – the vacuum aerodynamic diameter, χ_v – the shape factor in the free molecular regime, D_v – the aerodynamic diameter, ρ_p – density of the particles material, ρ_0 – 1 g cm^{-3}. Q-AMS provides the diameter expressed as the diameter of the sphere-shaped particle with the density of 1 g cm^{-3} that settles at the same velocity as the particle of interest.

Position of the chopper wheel determines whether the instrument is working in a mass spectrometer mode (MS) or in time of flight (TOF) mode. TOF provides the vacuum aerodynamic diameter described above whereas the mass spectrometer mode retrieves mass concentration spectra of the species presented within the captured particles. The total mass concentration *C* for a particular species *s* can be expressed using the following equation (Canagaratna et al., 2007):

$$C_s = \frac{10^{12} MW_s}{IE_s Q N_A} \sum_{all\,i} I_{s,i} \tag{2.2}$$

where C_s is expressed in μg m^{-3}, IE_s is the ionization efficiency of species s expressed in ions/molecule, $I_{s,i}$ are ions s^{-1}, N_A is the Avogadro's number, MW_s is the molecular weight of species s, and Q is the speed of ambient air flow into the Q-AMS in cm^3 s^{-1}.

Main characteristics of Q-AMS are: the lower limit of detection is 32 ng m^{-3}, the flow rate – 0.85 l min^{-1}, the measured *m/z* range is from 1 to 300. During the measurement campaigns the instrument was calibrated as required. The ionization efficiency was calibrated using 300 nm dry ammonium nitrate particles, owing to their ability of being reasonably well focused by the aerodynamic lens system and having a high efficiency of collection. The collection efficiency value (CE) during experiments was set at 0.5 (Middlebrook and Bahreini, 2008), and calibrations for the quadrupole mass, resolution and electron multiplier were performed.

2.2.2 Scanning Mobility Particle Sizer

Performance of the SMPS (Scanning Mobility Particle Sizer) analyzer is based on the mobility of the charged particles in the electric field. The instrument is used to obtain the aerosol size distribution. SMPS is composed of two main parts that are named as DMA (Differential Mobility Analyzer) and CPC (Condensation Particle Counter). For the accuracy, however it is necessary to note that in SMPS system so called neutralizer is also used, particles pass through it before entering DMA. DMA separates particles based on their electrical mobility and subsequently CPC is used to count emerging particles. The property of the particle being bend in the electric field is called the electrical mobility; therefore, it depends on the size of a particle and its state of charge. The DMA is a column shaped construction that consists of a

tube and a rod inside it (Fig. 2-5). A custom voltage is applied to a rod; hence difference between the voltage of the rod and that of the outer shell generates the electric field. Particles with the same size and charge hit the center rod together. Ones with the higher electrical mobility hit the rod at the faster rate than those of the lower electrical mobility. Flow inside the column is strictly only laminar. Only certain size and charge particles can be captured through the slit that is positioned at the bottom of the column since the applied voltage is related to the certain electrical mobility. Particles are sorted by the electrical mobility that is expressed as follows:

$$Z_p = \frac{n \cdot e \cdot C_c}{3 \cdot \pi \cdot \eta \cdot D_p} \tag{2.3}$$

Where Z_p – the electrical mobility, n – the charge of the particle, e - the elemental charge, C_c – the Cunningham factor of correction, η - viscosity of the air, D_p – the diameter of the particle.

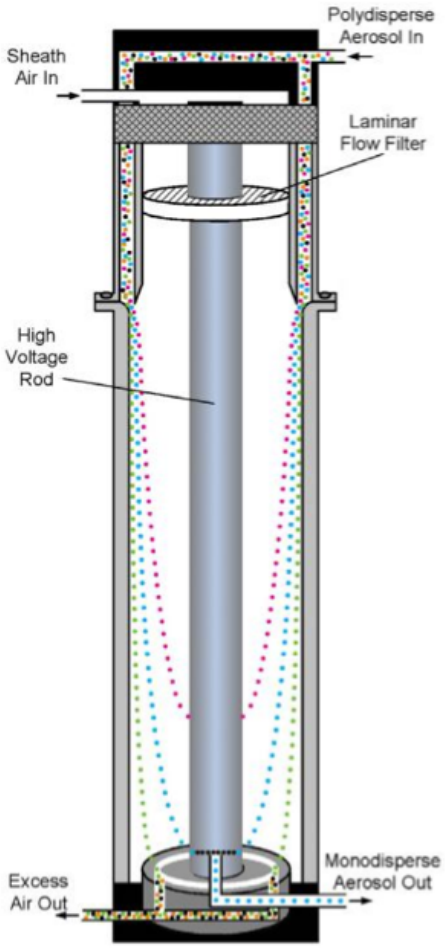

Fig. 2-5. Principle scheme of DMA (adopted from www.tsi.com)

The sorted mono-disperse particles emerging at the exit of DMA eventually enter CPC (Fig. 2-6). Once particles enter CPC they are grown by the vapor of the present working fluid (usually it is water, butanol, alcohol or isopropyl) up to the size so that they could be optically detected. The instrument detection limit is considered to be d_{50} (when the rate of particles detection is reduced to 50 % of all particles that could be detected). CPC calculation of the particle concentration for a certain period of time can be expressed as follows:

$$[Particles\ cm^{-3}] = [particles] \cdot (time\ [s] \cdot flow\ rate\ [ls^{-1}] \cdot 1000\ [cm^{-3}l])^{-1} \qquad (2.4)$$

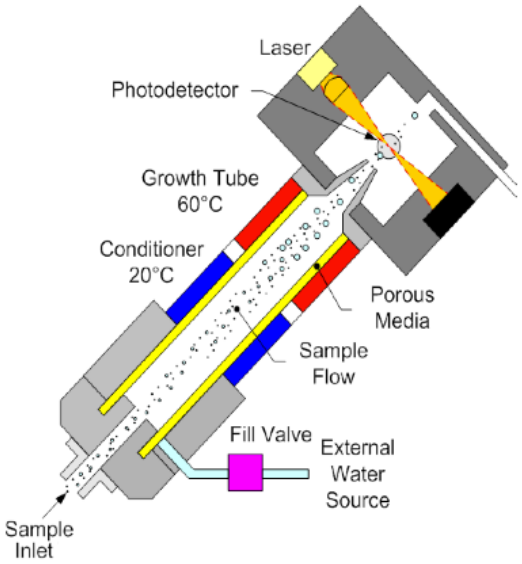

Fig. 2-6. Principle scheme of CPC (adopted from www.tsi.com).

DMA performs scan of the particles within a certain range of voltage and CPC counts sorted particles, accordingly. Thus, size distribution within a demanded range is obtained. SMPS provides a mobility diameter of the particles, which equals:

$$d = \sqrt[3]{\frac{6m}{\pi\rho}} \tag{2.5}$$

SMPS model N 19.3.09 IFT/TT produced by Leibniz Institute for Tropospheric Research was employed during the measurement campaign presented herein. Its main characteristics are: CPC working fluid – butanol, the size distribution interval: from 8.7 nm to 839.6 nm (Hauke medium DMA), the uncertainty of the measurement – 10 %, the concentration expressed as the number of particles in cm^3, sheath flow rate – 5 l min^{-1}, sample flow rate 1 l min^{-1}, resolution – 5 min, sizing channels – 71, during the measurement relative humidity did not exceed 50 %. It is important to remember that Q-AMS and SMPS measure different diameters (aerodynamic and electrical

mobility): $\rho d = \rho_0 D$, where ρ is the density of the particle; ρ_0 is the density of the water; d is the mobility diameter of the particle; D is the aerodynamic diameter measured with Q-AMS.

2.2.3 Air masses trajectory evaluation

The impact of long-range transport air masses was evaluated in the analysis of mass concentration, distribution of chemical compounds and source apportionment at the urban and background sites. The backward trajectory analysis was also applied in order to retrieve air mass trajectory of the volcanic pollutants that had reached the measurement site in Vilnius. The long-range air masses were defined by using the long-range transport air masses trajectory model – Hybrid Single Particle Lagrangian Integrated Trajectory Model – HYSPLIT model (Draxler and Rolph, 2014) provided by the National Oceanic and Atmospheric Administration (NOAA). The advected air mass trajectories were calculated every 6 hours with the backward duration of 72 hours at 50 m, 500 m and 1500 m above the ground level (AGL). Captured episodes of volcanic pollutants over Lithuania have shown that advected long-range air masses can have a noticeable influence on the local mass concentration and the particle size distribution up to 3000 km away from the emission source, thus the assessment of long-range transport air masses impact is rather important (Kvietkus et al., 2013).

2.2.4 PMF – Statistical evaluation method

Organic matter constitutes a significant fraction of all aerosol particles. It can comprise from 20 % to 90 % of all measured PM1 (Zhang et al., 2007). However, the source and origin characterization of this substantial fraction of aerosol particles is still poor. The idea to apply the Positive Matrix

Factorization (PMF) method (Paatero and Tapper, 1994; Paatero, 1997) on data of organic aerosol obtained with Q-AMS was put forward by Ulbrich et al. (2009). PMF method was adapted to the data obtained with Q-AMS (Ulbrich et al., 2009). PMF Evaluation Tool (PET) was created for the Igor-Pro software since Q-AMS data analysis is carried out in Igor-Pro software environment. Therefore, PMF Evaluation Tool (PET) was used hereafter. PMF method helps to solve the source apportionment task for organic matter captured with Q-AMS. The PMF method is applied to the organics component in order to obtain the source apportionment information. Data in Q-AMS are stored in the form of convolved matrix. The main idea of the method is to deconvolve matrix of organic mass spectra into a few separate matrixes. Result of deconvolution yields a number of separate mass spectra matrixes that have their own mass spectra, time series and eventually a residual matrix is left (Fig. 2-7). Resulted mass spectra are called factors.

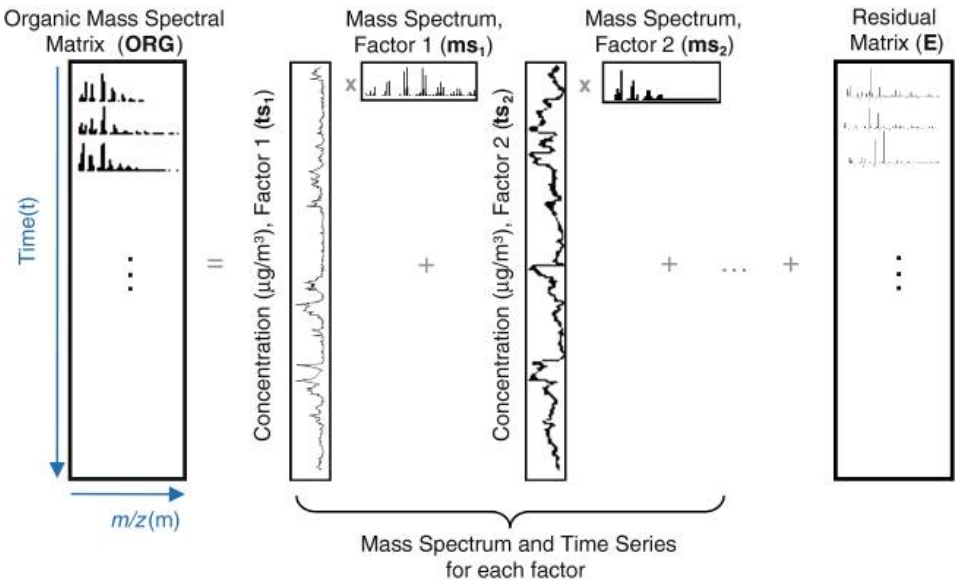

Fig. 2-7. Scheme of how Q-AMS stores organic matter matrix information. Picture taken from (Zhang et al., 2011).

The smaller the residual matrix and the larger the number of factors, the better the accuracy is achieved, although PET user decides how many factors to choose, and this is a drawback of this technique. One should be aware and cautious for the uniqueness of the retrieved factors. It is rather important to adhere to the uniqueness and stability rule because it is the crucial for appropriate and reliable source apportionment.

The PMF method was run by altering the number of factors from 1 to 7 in this study. The minimum value of residual matrix was obtained while stable and unique factors were generated. During analysis, a final number of factors was chosen based on the stability and uniqueness of the recognized factors for each organic component from Vilnius, Rūgšteliškis and Preila sites, accordingly.

2.3 Chapter conclusion

On-line measurement instruments with ability to provide real time information on aerosol particles became available at the very end of the last century, a few decades ago. The ability to provide real-time information on ambient aerosol particles is the most important and valued feature of the employed measurements instrument ever since. Possibility to conduct online measurements helped to save a lot of time inevitably used for collecting samples and processing them in the laboratory. More importantly real time measurement enables obtaining preciseness in raw data. The drawback of the sampling technique with the filters is that the part of the aerosol particles collected on the filters is lost before captured and registered in the laboratory with immobilized spectrometric instruments. The spectrometer used in this study is one of the most modern devices used in Lithuania for aerosol particle observation and analysis. AMS spectrometer has several modifications; the one

with a quadrupole is used for this study. Data from rural, urban and coastal sites are obtained and analyzed.

3 RESULTS

This chapter presents results of analysis from conducted measurements. Analysis is divided into three main parts: i) PM1 characterization including the estimation of ammonium nitrate and ammonium sulfate mass contribution to the total of ammonium; ii) analysis of PM1 organic matter density within a aerosol particle at an urban site; iii) the extent of natural neutralization of acidic sulfate particles with atmospheric ammonia in volcanic origin aerosol particles during long-range transport.

3.1 Characterization of PM1 at urban and background sites in Lithuania

3.1.1 The average mass concentration of PM1 chemical components

Mass concentration measurements of semi-volatile non-refractory components in submicron particles showed that the highest average PM1 concentration value of 7.69 ± 0.08 μg m^{-3} was observed at the Vilnius site, lower concentrations of 4.19 ± 0.03 μg m^{-3} and 3.44 ± 0.03 μg m^{-3} at the Rūgšteliškis and Preila site, respectively. The average percentage mass concentration of PM1 chemical components at all three sites shows that organics is a dominant component (68.8 % – 77.1 %) of the captured volatile and semi-volatile non-refractory compounds in PM1 aerosol volume at all three sites (Fig. 3-1). It is consistent with the previous results of our laboratory where organics made up from 74.1 % to 82.7 %, 60 % and 80 % of the total volatile and semi-volatile non refractory compounds in PM1 mass, respectively (Garbariene et al., 2012; Kvietkus et al., 2011; Rimselyte et al., 2007). These

data indicate that organics accounts for about 70% of all PM1 in aforementioned sampling sites during mild season.

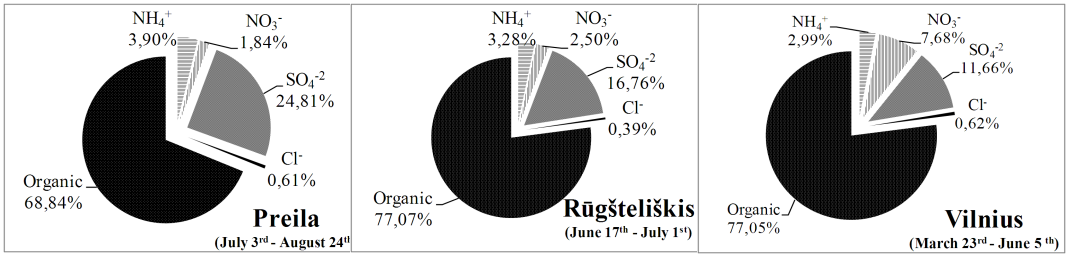

Fig. 3-1. Average percentage concentrations of volatile and semi-volatile non-refractory PM1 chemical components at the Vilnius, Rūgšteliškis and Preila sites.

It is more likely that a significant fraction of organics at the background sites was advected with air masses or emitted from biogenic sources such as sea spray at the Preila site or reactive terpenes at the Rūgšteliškis site (Finessi et al., 2012; Gantt et al., 2011) during the analyzed periods. In urban areas, PM1 was mainly composed of primary particles of anthropogenic origin and secondary particles produced by formation from ambient primary pollutants (Dall'Osto et al., 2006; Kvietkus et al., 2011). The percentage mass concentration of nitrate in Vilnius was three-fold higher than at Rūgšteliškis and four-fold higher than at the Preila site. Stagnant conditions and low mixing height due to the low wind speed (up to 3 m s^{-1}) had caused negligible dissipation during the sampling period in Vilnius, therefore, the concentration was higher than usual level. Secondly, the increased nitrate concentration in Vilnius was observed at the north-east wind, while the mass concentration was reduced at the north-west wind, suggesting the influence for nitrates from transportation sources (O'Dowd et al., 2012). Moreover, Vilnius city is under the influence of local pollution sources such as the power plant situated to the east of the sampling site.

3.1.2 Mass concentration dependence on the origin of the air masses

Air mass backward trajectories were calculated using the HYSPLIT model. The trajectories of air masses were divided into 8 sectors, and those with uncertain origin (originated in 3 or more sectors) were rejected. Over 4800 backward trajectories were retrieved and evaluated for all sampling sites out of which 1951 were for Vilnius site (11 % rejected as not stable), 588 trajectories at the Rūgšteliškis (no rejection, all stable), 1782 at the Preila site (14 % were rejected as not stable with unclear origin) (Table 3-1).

Table 3-1. Statistics of the air masses trajectories.

	Vilnius	Rūgšteliškis	Preila
N	526	57	165
NE	45	36	6
E	191	76	188
SE	36	0	57
S	156	25	208
SW	260	186	550
W	117	47	188
NW	620	161	420
Total	1951	588	1782
Rejected	244 (11 %)	0	294 (14 %)

Fig. 3-2 depicts the dependence of the mass distribution of PM1 chemical components (chloride, ammonium, nitrate, sulfate and organics) on air mass trajectories at the three sites (note – ammonium and organics concentration is shown by half of it for the convenience). The peak mass concentration for all PM1 components was observed in the presence of air masses from the south and south-east in Vilnius (Fig. 3-2).

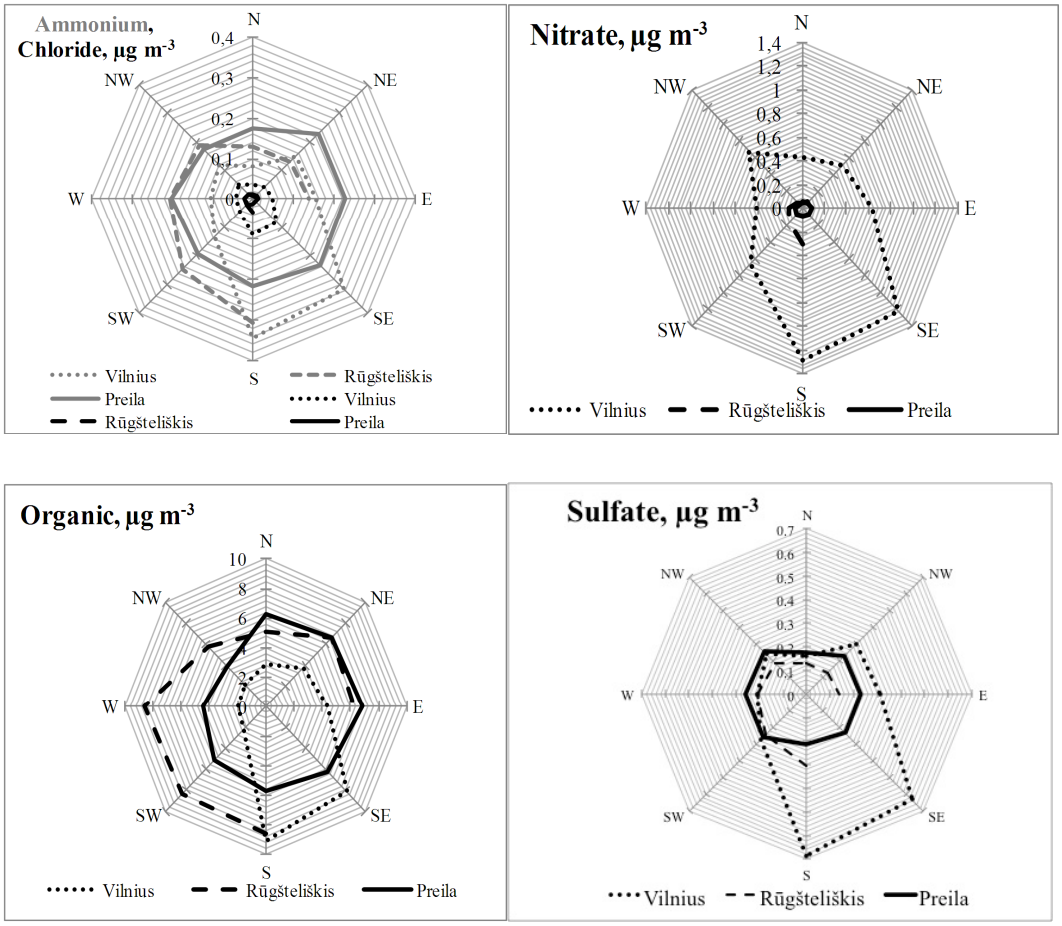

Fig. 3-2. Dependence of ammonium, chloride, sulfate, nitrate and organics mass concentrations on backward air mass trajectories.

During the same period, local wind directions from the east and north-east were dominant at the Vilnius site, and the local pollution input could not be clearly quantified, either it was due to air masses or wind direction at the Vilnius site. The peak concentration at the Rūgšteliškis site was observed with advected air masses from the south, while increased concentrations were observed with north-east and south-east air masses at the Preila site. Sulfate was the exception at Preila site as the concentration increased with air masses from the sea (south-west, west and north-west), suggesting that the increased concentration of sulfates was due to marine aerosol particles.

3.1.3 Nitrate and sulfate contribution to the total of ammonium

Nitrate, sulfate and ammonium are the most abundant inorganic species of the secondary aerosol particles in the submicron range, although nitrate is found to be bi-modal with present in fine and coarse modes. Formation of ammonium sulfate containing aerosol particles is likely to decline and on the contrary that of nitrate to increase due to increased precursors according to future predictions. The effect of nitrate aerosols will become more important. The system of nitrate, sulfate and ammonium behaves rather complicated in natural environment. Nitric and sulfur acid aerosol particles compete for the ammonia present in the atmosphere. Formation of ammonium nitrate is closely related with the thermodynamic state of its precursors and ambient conditions. A number of models presume that ammonia (gas phase) instantly reaches equilibrium with ammonium (aerosol phase) in a submicron range, whereas for coarse particles it rather might take up to a few days to reach the equilibrium. Analysis of Q-AMS measured nitrate and sulfate allowed quantifying the ammonium nitrate and ammonium sulfate contribution to the total mass of captured ammonium in a submicron range.

The average mass concentration of ammonium was similar at Rūgšteliškis and Preila (0.14 μg m^{-3} and 0.13 μg m^{-3}, respectively), nevertheless the median diameter for the accumulation mode of ammonium was higher at the Preila site (Fig. 3-3) than at Vilnius site, therefore meaning different particle sources and formation processes at the background and urban sites (Seinfeld and Pandis, 1998).

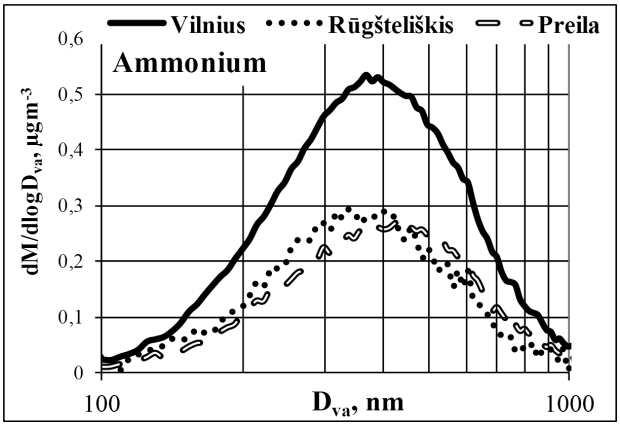

Fig. 3-3. Modes of ammonium at the sampling sites.

The difference in the median diameter could be explained in terms of growth promotion by water uptake of ammonium particles at the Preila background site, which is consistent with data reported in the study by Seinfeld et al. (2001) where an increase in the secondary aerosol mass induced by the increase of relative humidity is analyzed. Furthermore, particle formation is also enhanced by the water uptake of fine particles as some compounds forming secondary aerosol particles are water-sensitive (Pun and Seigneur, 2007; Hennigan et al., 2008).

Q-AMS is a quantitative instrument for measurements of non-refractory ammonium, even though Q-AMS cannot distinguish and quantify the contribution of different compounds to the total quantity of certain components (e.g. which part of the ammonium is from ammonium nitrate and which is from ammonium sulfate). In this study the variance in nitrate and sulfate mass concentrations is used to evaluate the contributions of ammonium nitrate out of all nitrates and ammonium sulfate out of all sulfates to the total quantity of ammonium captured with Q-AMS. Concentration of nitrate and sulfate correlates with the concentration of ammonium (Fig. 3-4); therefore variance of nitrate and sulfate concentrations is used to determine their quantity in ammonium compound captured by Q-AMS. Fig. 3-4 depicts mass concentration variance in the period of April 2-8 at the Vilnius sampling site

for nitrate, sulfate and ammonium. The least squares method is applied to concentration data of ammonium, sulfate and nitrate. Calculations are expressed as follows:

$$C_{NH_4^+} = AC_{NO_3^-} + BC_{SO_4^{2-}} \tag{3.1}$$

$$\begin{cases} A\sum_{i=1}^{n} C_{NO_3^-}^2 + B\sum_{i=1}^{n} C_{NO_3^-} C_{SO_4^{2-}} = \sum_{i=1}^{n} C_{NH_4^+} C_{NO_3^-} \\ A\sum_{i=1}^{n} C_{NO_3^-} C_{SO_4^{2-}} + B\sum_{i=1}^{n} C_{SO_4^{2-}}^2 = \sum_{i=1}^{n} C_{NH_4^+} C_{SO_4^{2-}} \end{cases} \tag{3.2}$$

Solving equation (3.2) yields coefficient of ammonium nitrate (A) and that of ammonium sulfate (B) contributions to the total of captured ammonium. Coefficients A and B denote the contribution of ammonium nitrate and ammonium sulfate if the contribution of those to ammonium was 100 %. Ratio of the coefficient A versus molar ratio of ammonium to nitrate indicates contribution rate of ammonium nitrate out of all nitrates. Contribution of ammonium sulfate is retrieved in the same way. Chloride was not considered firstly due to its relatively low concentration compared to that of sulfate, and secondly because ammonium nitrate formation is dominant when compared to ammonium chloride (Du et al., 2010).

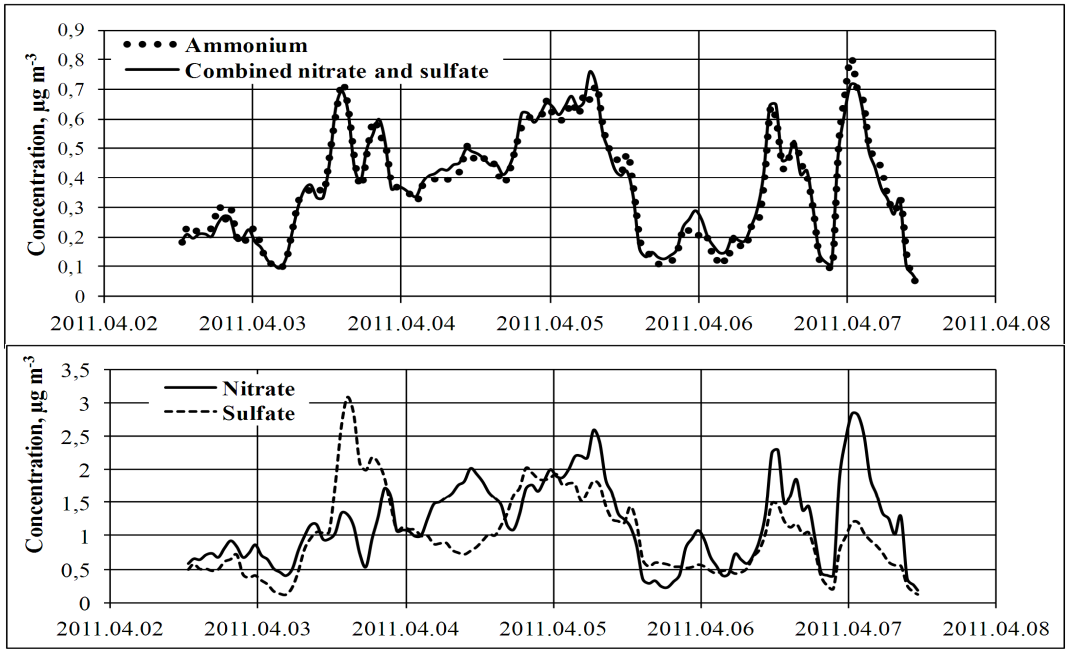

Fig. 3-4. Nitrate, sulfate and ammonium concentrations (measured) and combined nitrate and sulfate concentrations as ammonium concentration.

Initially, it was expected that ammonium sulfate would make a relatively greater contribution to the overall quantity of ammonium compared to ammonium nitrate. On the contrary, this study has indicated that ammonium nitrate out of all nitrates (on the average 61 % at the Vilnius and Rūgšteliškis sites and 80 % at the Preila site) made a greater contribution than that of ammonium sulfate out of all sulfates (37 %, 44 % and 36 % for the Vilnius, Rūgšteliškis and Preila sites, respectively) (Table 3-2).

Sulfuric acid is indicated as the main driver of the secondary aerosol particles formation, but the role and impact of other components have been not clearly understood yet (O'Dowd et al., 1999). Therefore, results of this study shows that it is not proper to consider sulfuric acid components to be the sole agent for the secondary aerosol formation.

Table 3-2. Percent contribution of ammonium nitrate (out of all nitrates) and ammonium sulfate (out of all sulfates) to the total quantity of ammonium, and the average molar concentrations of nitrate, sulfate and ammonium.

Date and location	NH_4NO_3 %	$(NH4)_2SO_4$ %	NO^-_3 µmol m^{-3}	SO^{-2}_4 µmol m^{-3}	NH^+_4 µmol m^{-3}
Vilnius					
2011.03.23 / 03.28	63	44	0.0031	0.0026	0.0043
2011.03.28 / 04.01	70	44	0.0138	0.0080	0.0166
2011.04.02 / 04.07	66	38	0.0193	0.0104	0.0206
2011.04.07 / 04.18	70	33	0.0155	0.0092	0.0165
2011.04.18 / 04.22	54	40	0.0076	0.003	0.0063
2011.04.22 / 05.04	56	37	0.0149	0.0256	0.0274
2011.05.04 / 05.13	44	38	0.0071	0.0081	0.0092
2011.05.13 / 05.19	70	30	0.0039	0.0075	0.0071
2011.05.24 / 05.26	57	33	0.0008	0.0096	0.0067
Average	**61** ± 9	**37** ± 5	**0.0096**	**0.0093**	**0.0127**
Rūgšteliškis					
2011.06.17 / 06.24	65	45	0.0026	0.0098	0,0107
2011.06.24 / 07.01	58	43	0.0009	0.0053	0,0051
Average	**61** ± 5	**44** ± 2	**0.0017**	**0.0075**	**0,0079**
Preila					
2011.07.03 / 07.16	100	35	0.0011	0.0106	0,0089
2011.07.16 / 07.27	55	39	0.0009	0.0100	0,0084
2011.07.31 / 08.08	34	36	0.0011	0.0084	0,0064
2011.08.08 / 08.18	66	34	0.0009	0.0065	0,0050
2011.08.18 / 08.24	100	39	0.0011	0.0090	0,0085
Average	**80** ± 3	**36** ± 2	**0.0010**	**0.0089**	**0,0074**

It is important to note that ammonia in the boundary layer is in the gas phase and is converted into particulate matter at higher altitudes, where the dissociation constant of ammonium nitrate decreases due to the low ambient temperature (Neuman, 2003). Ternary H_2SO_4-NH_3-H_2O nucleation is important to the secondary aerosol formation in the boundary layer (Merikanto et al., 2009), and, according to the study of Kirkby et al. (2011), H_2SO_4-H_2O nucleation is insignificant in the boundary layer due to uniformly-distributed oxidized sulfuric compounds. However, H_2SO_4-H_2O nucleation is dominant in the mid-troposphere. Nucleation and secondary aerosol formation processes are not fully understood and are still under discussion (Merikanto et al., 2009).

Presented observations could be explained as follows: i) the reaction between single-phase components is much more likely to occur than between multi-phase components (3.3); ii) the growth of particles favors ammonium nitrate formation, iii) nucleation processes, iv) the uptake of ammonia into acidic aerosols contributes to the formation of ammonium nitrate, and v) local conditions strongly influence nitrate aerosol formation as a result of abundant precursor gases in ambient air (Xu and Penner, 2012).

$$NH_{4(g)} + HNO_{3(g)} \leftrightarrow NH_4NO_3 \qquad (3.3)$$

During the period presented in Fig. 3-4 wind conditions were stagnant (average wind speed was about 0.7 m s^{-1}) and the western wind direction was predominant. The average temperature was about 6.3ºC with the 73 % relative humidity (RH). The long-range air masses on April 2-8 were unstable (NW, W, SE, S, W, NW and NW), hence the influence of long-range air masses was minor. The molar concentrations for nitrate, sulfate and ammonium are presented in Table 3-2. The nitrate molar concentration is nine-fold lower at the Preila site compared to the Vilnius site, sulfate molar concentration is comparable at all three sampling sites and the ammonium molar concentration was nearly two-fold lower at the background sites compared to the urban site. The same calculations as for period of April 2-8 were performed to the data from all measurement sites (Vilnius, Rūgšteliškis, Preila). Local conditions of the other sampling sites showed no influence on calculations, similar results as shown in Fig. 3-4 was obtained.

3.1.4 Positive Matrix Factorization analysis to organic matter

The Positive Matrix Factorization (PMF) method developed by (Paatero and Tapper, 1994) is used to obtain origin apportionment of organic compounds. A solution of three factors is consistent with the chosen criteria (stability and uniqueness) at the Vilnius and Rūgšteliškis sites (Q/Q_{exp} = 1.3,

Q/Q_{exp} = 0.56, respectively), and a solution of two factors at Preila site (Q/Q_{exp} = 0.92).

Three factors are indicated at the urban sampling site in Vilnius: BBOA (32 %), HOA (28 %) and SV-OOA 40 %) (Fig. 3-5). The most distinctive tracers of BBOA are *m/z* = 60 ($C_2H_4O_2^+$) levoglucosan and *m/z* = 73 ($C_3H_5O_2^+$). These tracers were identified in this case of study. The value of f_{60} was 0.01 higher when compared to its value of other factors, thus the presence of the BBOA factor implies the influence of biomass burning emissions in Vilnius (f_{60} is the ratio of *m/z* = 60 to the total organics in the mass spectrum of the factor).

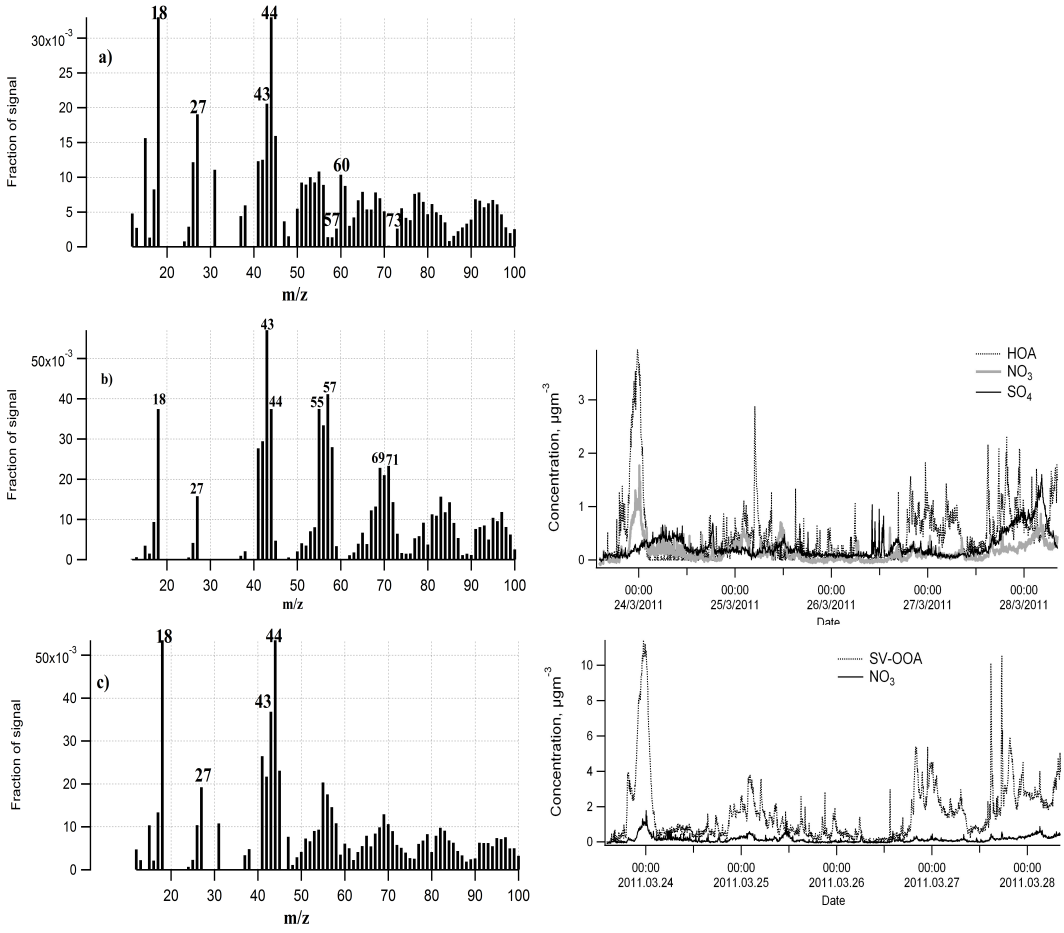

Fig. 3-5. a) BBOA factor *m/z* spectra, b) HOA factor *m/z* spectra and time series with tracers and c) SV-OOA factor *m/z* spectra and time series with tracer at the Vilnius site.

The HOA factor is identified due to the presence of f_{57}, assumed as the most valuable indicator of HOA. The f_{57} value is close to the reference spectrum value (f_{57} = 0.04), while other *m/z* values for the standard HOA spectrum (27, 41, 43, 55, 57, 69, 71, 83, 85, 97) are observed with the tracers of nitrate (r = 0.65, N = 1370) and sulfate (r = 0.14, N = 1370) particulate matter. The SV-OOA profile has the f_{44} value of 0.05, the same f_{44} value is reported in the study of Malloy et al. (2009). The f_{44} value is highest in the SV-OOA spectrum when compared to other factors, thus indicating that SV-OOA consists of more-oxygenated organics than HOA (f_{44} = 0.04) and BBOA (f_{44} = 0.03), although, however, SV-OOA profile correlates with its tracer, particulate

nitrate (Fig. 3-5) (r = 0.76, N = 1370), indicating a relatively higher contribution of fresher secondary aerosol particles than that of aged secondary aerosol particles (r (SV-OOA – SO_4) = 0.14, N=1370) (Ulbrich et al., 2009).

During the period of June 17-24, three factors (BBOA – 32 %, LV-OOA – 21 %, SV-OOA – 47 %) are indicated at the Rūgšteliškis background sampling site, Fig. 3-6. It is likely that the BBOA factor increased due to the bonfires in Lithuania and neighboring Latvia during the national holidays (June 21-24). The f_{44} values for SV-OOA and LV-OOA are calculated to be equal to 0.02 and 0.18, respectively, relatively close to the values of 0.05 and 0.16 as reported in Ng et al. (2011). The lower contribution of m/z = 44 suggests that the particles of SV-OOA factor are less oxygenated and fresher than LV-OOA particles at Rūgšteliškis site. The LV-OOA time-series correlates with the sulfate particulate (r = 0.42, N = 2043), this is similar to that reported in Kvietkus et al. (2011), while the SV-OOA time series correlates with particulate nitrate (r = 0.25, N = 2043) (Fig. 3-6 b, c). The biogenic m/z = 27 tracer is observed for BBOA and SV-OOA, with f_{27} = 0.01 for both factors.

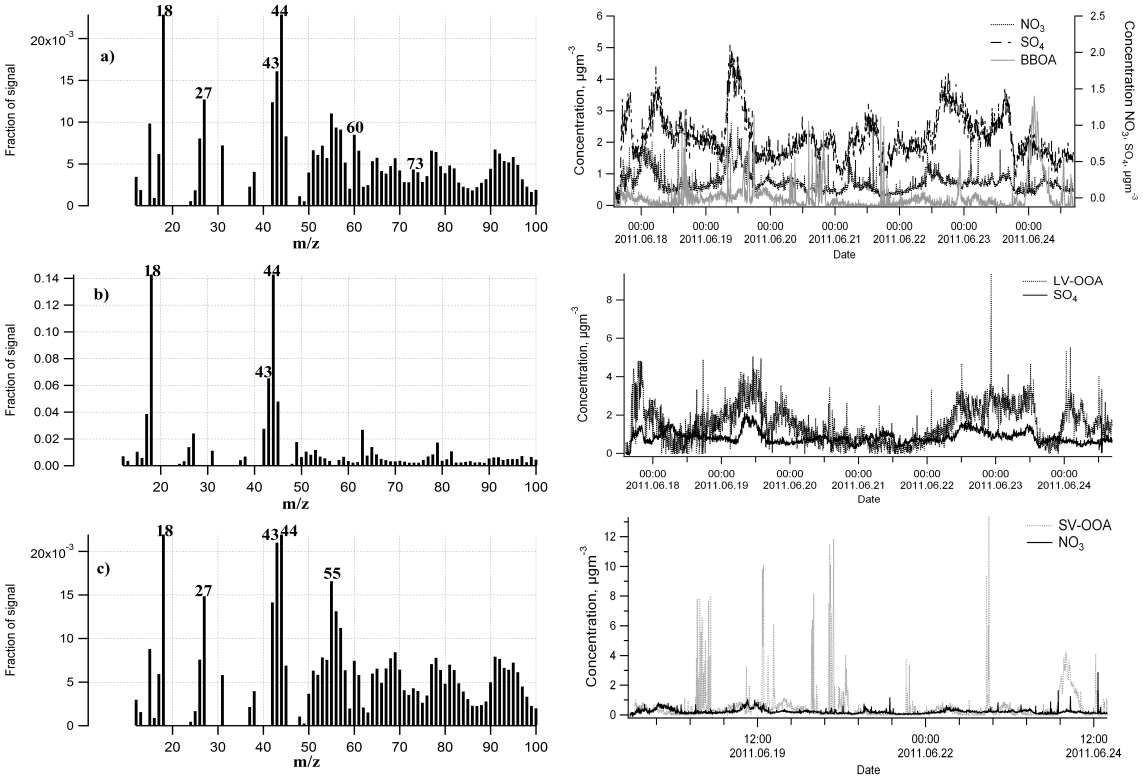

Fig. 3-6. BBOA, LV-OOA, SV-OOA factors indicated at the Rūgšteliškis site.

Two factors (LV-OOA and SV-OOA) comprising 64 % and 36 % to the total organic mass, respectively, are identified at the background site of Preila, (Fig. 3-7). It is likely that the factor of BBOA is negligible due to the seasonal conditions. LV-OOA and SV-OOA factors are similar to those reported in the study of Garbariene et al. (2012), however one must be cautious when evaluating the contribution of factors due to the contrary results reported for this site, where LV-OOA contributed 22% and SV-OOA 63% to the total organic mass (Garbariene et al., 2012). LV-OOA correlates with particulate sulfate (r = 0.63, N = 1657) and SV-OOA correlates with particulate nitrate (r = 0.62, N = 1657). It should be noted that SV-OOA factors with values of *m/z* = 18, 27, 41, 43, 44, 55, 58, 60, 69, 79, 83, 91 are very similar to those reported/defined as the BGOA factor in Garbariene et al. (2012) and Ovadnevaite et al. (2012). The SV-OOA f_{44} values at the Preila and Rūgšteliškis sites are 0.18, suggesting that this ratio might be typical of the f_{44}

value of SV-OOA for background sites, however further experiments are required to confirm this assumption.

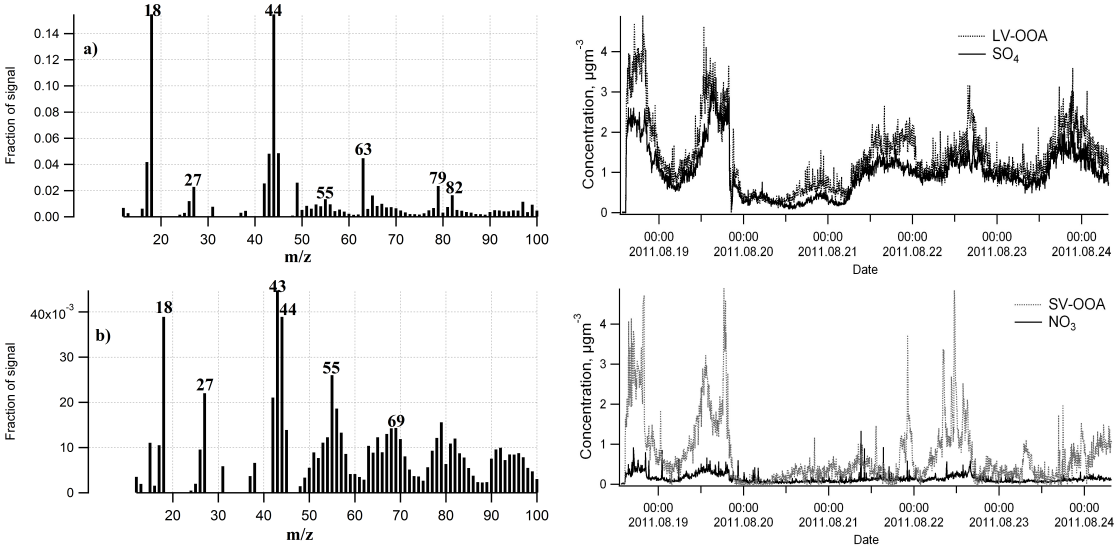

Fig. 3-7. LV-OOA and SV-OOA factors identified at the Preila site.

3.1.5 Conclusion

It is shown that organics is the most abundant component at all three sampling sites, accounting from 68.8 % to about 77.1 % of the total measured PM1 mass concentration in Lithuania during a mild season. PM1 mass concentration comprised 68.8 % at the Preila site, whereas 77.0 % and 77.1 % at the Vilnius and Rūgšteliškis sites respectively, suggesting that concentration of organics was determined by the biomass burning emissions from bonfires during national festival on the 23th – 24th of the June at the Rūgšteliškis site.

The concentration of nitrates at the urban Vilnius site is four-fold higher than that at the background Preila site and three-fold higher than that at the background Rūgšteliškis site (7.68 %, 1.84 % and 2.50 % respectively). The increased PM1 concentration in Vilnius correlates with the north-east (directly from the city center) wind direction, while a rapid increase in PM1 concentration was observed when air masses prevailed from the east in

Rūgšteliškis and for north-east/south-east air masses in Preila. It indicates that Vilnius city is under the severe influence of traffic-related nitrates, whereas Preila and Rūgšteliškis are influenced by advected long-range air masses.

The advantage of component mass concentrations variance (ammonium, sulfate and nitrate) was used in order to indicate which parts of sulfate and nitrate in aerosol particles are ammonium sulfate and which part is ammonium nitrate. Due to uniformity in the components phase, particle growth processes, particle nucleation and local conditions ammonium nitrate (on the average 61 ± 9 %, 61 ± 5 %, 80 ± 3 % Vilnius, Rūgšteliškis, Preila sites, respectively) the contribution out of all nitrates was higher when compared to that of ammonium sulfate (on the average 37 ± 5 %, 44 ± 2 %, 36 ± 2 % Vilnius, Rūgšteliškis, Preila sites, respectively).

PMF analysis revealed three factors at Vilnius site: BBOA (32 %), HOA (28 %), SV-OOA (40 %); three factors at Rūgšteliškis site: BBOA (32 %), LV-OOA (21 %), SV-OOA (47 %); two factors at Preila site: LV-OOA (64 %), SV-OOA (36 %). Preila and Rūgšteliškis sites are confirmed to be background sites, where less-oxygenated and fresher particles dominate. The typical value of f_{44} in SV-OOA at backgrounds sites is likely to be about 0.18, but it must be confirmed by further investigation.

3.2 Urban PM1 particulate matter density evaluation

Data from the measurement campaign in Siauliai town are analyzed in regard to the PM1 matter density. Measurement data from 15 March to 27 March, 2012 were divided into two periods: the first period (the short period) was from 6 pm on 15 March till 6 pm on 19 March and the second period (the long period) was from 6 pm on 19 March till 3 pm on 27 March (Fig. 3-8).

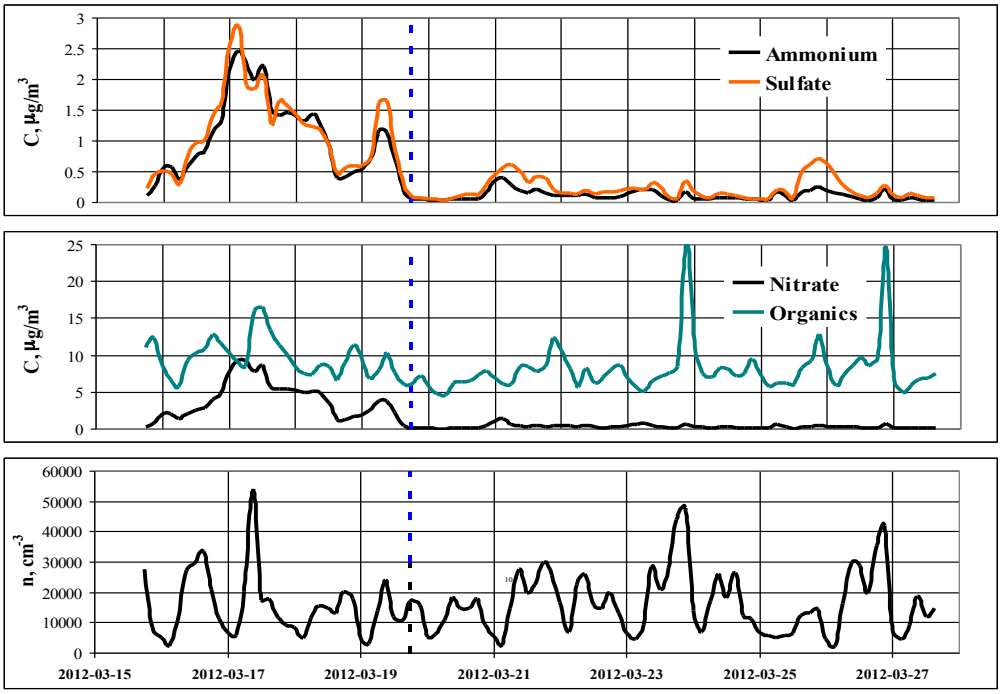

Fig. 3-8. The time series of NH_4^+, NO_3^- SO_4^{2-}, organics mass concentration and aerosol particles number concentration during the measurement campaign.

Partition is considered because concentrations of ammonium, nitrate and sulfate were higher from the beginning of the measurement till 6 pm on 19 March and relatively lower afterwards. The impact of the chloride concentration was not considered due to its low and widely scattered values.

During the short period predominant air masses had passed over France, Germany and northern parts of Poland, whereas during the long period air masses prevailed only from northern or north-western directions. Data of the measurement were also divided into nighttime and daytime sets regarding a relatively low impact of transport emissions during the nighttime (from 9 pm to 3 am) and on the contrary, a high impact of transport emission during the daytime (from 6 am to 9 pm). The obtained data sets were averaged over the short and the long measurement periods of air mass advection (Fig. 3 9). The long daytime period was chosen for analysis due to the lower concentration of NH_4^+, NO_3^-, SO_4^{2-} and the highest concentration of organics for the particles

with the diameter below 100 nm when compared to that during a short period. The latter size range was selected particularly because particles in this range mostly consist of hydrophobic organics emission from transport, while the other chemical components are negligible. It was assumed that the main source of organics was transport emissions due to the location of the measurement site. The assumption was confirmed by the high level of NO_x concentration at the measurement site (47.3 μg m^{-3} ± 3.6 μg m^{-3}) when compared to its usual background level (data from background station in Preila – 1.3 ± 0.2 μg m^{-3}). The density of particles organic matter was analyzed only for the particles with the diameter below 100 nm, because particles with the diameter of over 100 nm consist of hydrophobic and hydrophilic components, furthermore they could be formed either under the influence of urban pollution or long-range transport, and hence one should be aware of the humidity variation.

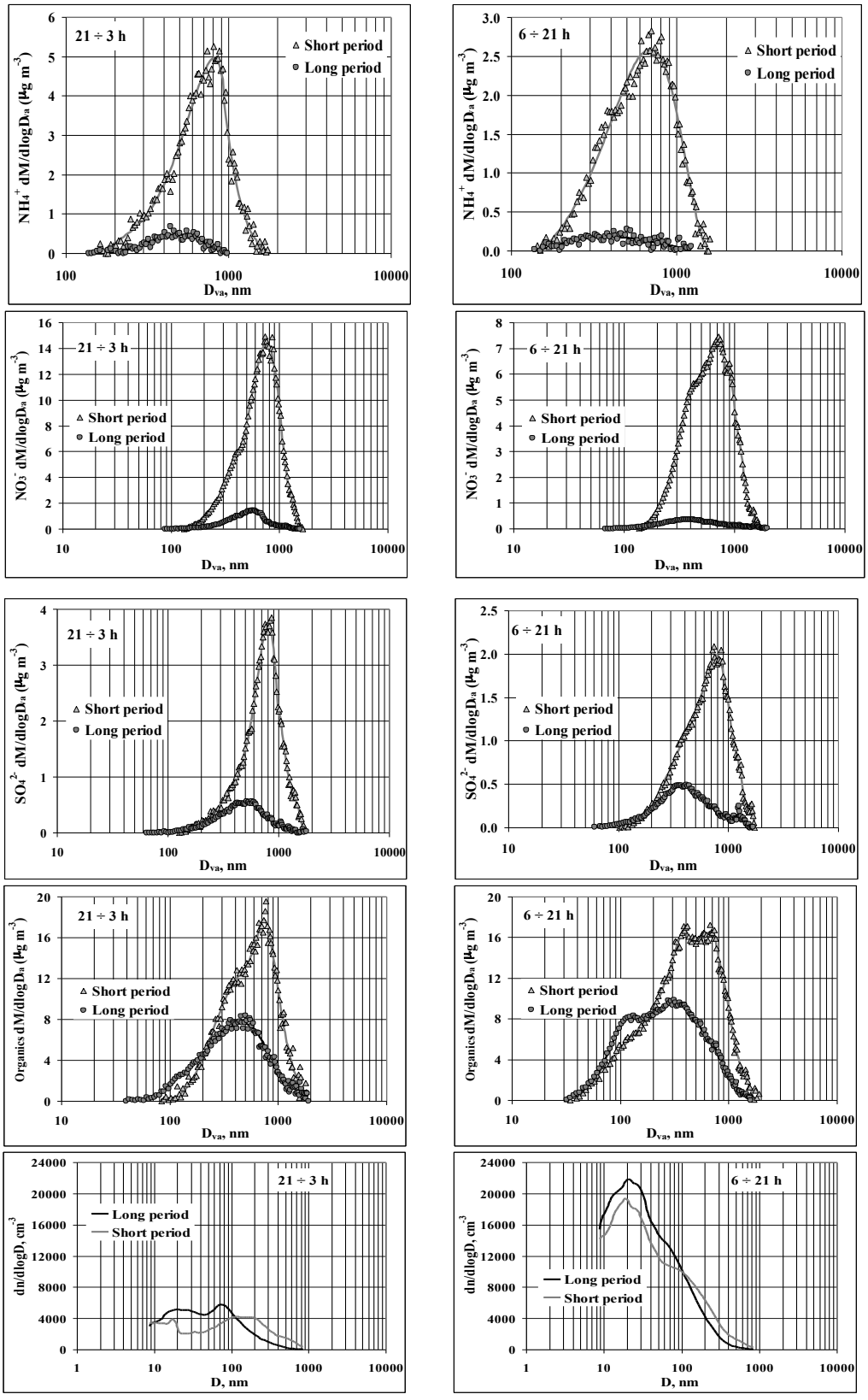

Fig. 3-9. NH_4^+, NO_3^-, SO_4^{2-}, organics and aerosol particles number concentration during a short and long period of the measurement.

3.2.1 The evaluation of submicron aerosol particle matter density

Q-AMS recognizes particles with the diameter $D_{va} = \frac{\rho(D_{va})}{\rho_0} SD_m$ as if they had the same diameter, thus $\rho_0 D_{va} \approx \rho(D_{va})D$, where ρ_0 is the density of the water (1 g cm^{-3}), D_{va} is the particle diameter according to Q-AMS; $\rho(D_{va})$ is the actual particle density, D is the actual particle diameter assuming that Jayne Shape Factor $S \approx 1$ when particles are spherical (Zhang et al., 2005).

In order to compare aerodynamic diameters provided both by Q-AMS and SMPS the resultant density of the particles was deducted:

$$\rho(D_{va}) = \frac{\sum_{i=1}^{n} m_i(D_{va})}{\sum_{i=1}^{n} \frac{m_i(D_{va})}{\rho_{0i}}} \tag{3.4}$$

Where $m_i(D_{va})$ is the mass of the component i for particles with the diameter D_{va}, ρ_{0i} is the material density of the component i.

Accordingly from the actual particle density, $\rho(D_{va})$, the actual diameter of the particle can be derived as follows:

$$D = \frac{\rho_0 D_{va}}{\rho(D_{va})} \tag{3.5}$$

Q-AMS provides $\frac{dm_i}{d\log D_{va}}$, thus a following correction is required:

$$\frac{dm_i}{d\log D} = \frac{dm_i}{d\log D_{va}} \cdot \frac{\Delta\log(D_{va})}{\Delta\log D} \tag{3.6}$$

SMPS provides:

$$\frac{d_n}{d\log D} \tag{3.7}$$

By using (3.6) and (3.7) expressions the concentration of the component i for the particles with the diameter D can be expressed:

$$C_i = \frac{\frac{d_m}{d\log D}}{\frac{\pi D^3}{6} \cdot \frac{dn}{d\log D}} \quad (3.8)$$

where $\frac{\pi D^3}{6}$ is the particle volume.

Here it is assumed that particles with the same size have the same density. Density values of chemical compounds were used as the ones reported in Mohr et al. (2012) as follows: NH_4^+ – 1.75 g cm^{-3}, NO_3^- – 1.72 g cm^{-3}, SO_4^{2-} – 1.78 g cm^{-3}, Cl^- – 1.4 g cm^{-3}, organics – 1.27 g cm^{-3}. During the experiment, the elemental carbon (EC) was not measured. For the organic carbon (OC) content evaluation the literature data containing an organic mass and organic carbon (OM / OC) ratio were used (Turpin and Lim, 2001; Xing et al., 2013). According to the literature data, this ratio is equal to 1.5. For the assessment of the EC content, data of the elemental to total carbon (EC / TC) ratio from an internal combustion engine exhaust gases are used (Gan et al., 2011), considering that TC = OC + EC. Knowing the amount of OM and using these relationships, the OC amount, and then the EC amount is obtained. The EC density is considered to be equal to 1.77 g cm^{-3} (Zhang et al., 2005). This theoretically derived contribution was considered to be extreme, because the OC / EC ratio of the internal combustion engine exhaust gases was used. In the aforesaid manner the density of NO_3^-, SO_4^{2-} and organics in the aerosol particle mass, including and not including EC, was deducted (Fig. 3-10). NH_4^+ was not analyzed due to its highly scattered values. As seen from Fig. 3-10 the daytime density of organics for the particles with the diameter below 100 nm is relatively too high when compared with the density sum of all components in the range above 100 nm (less than 1 g cm^{-3}).

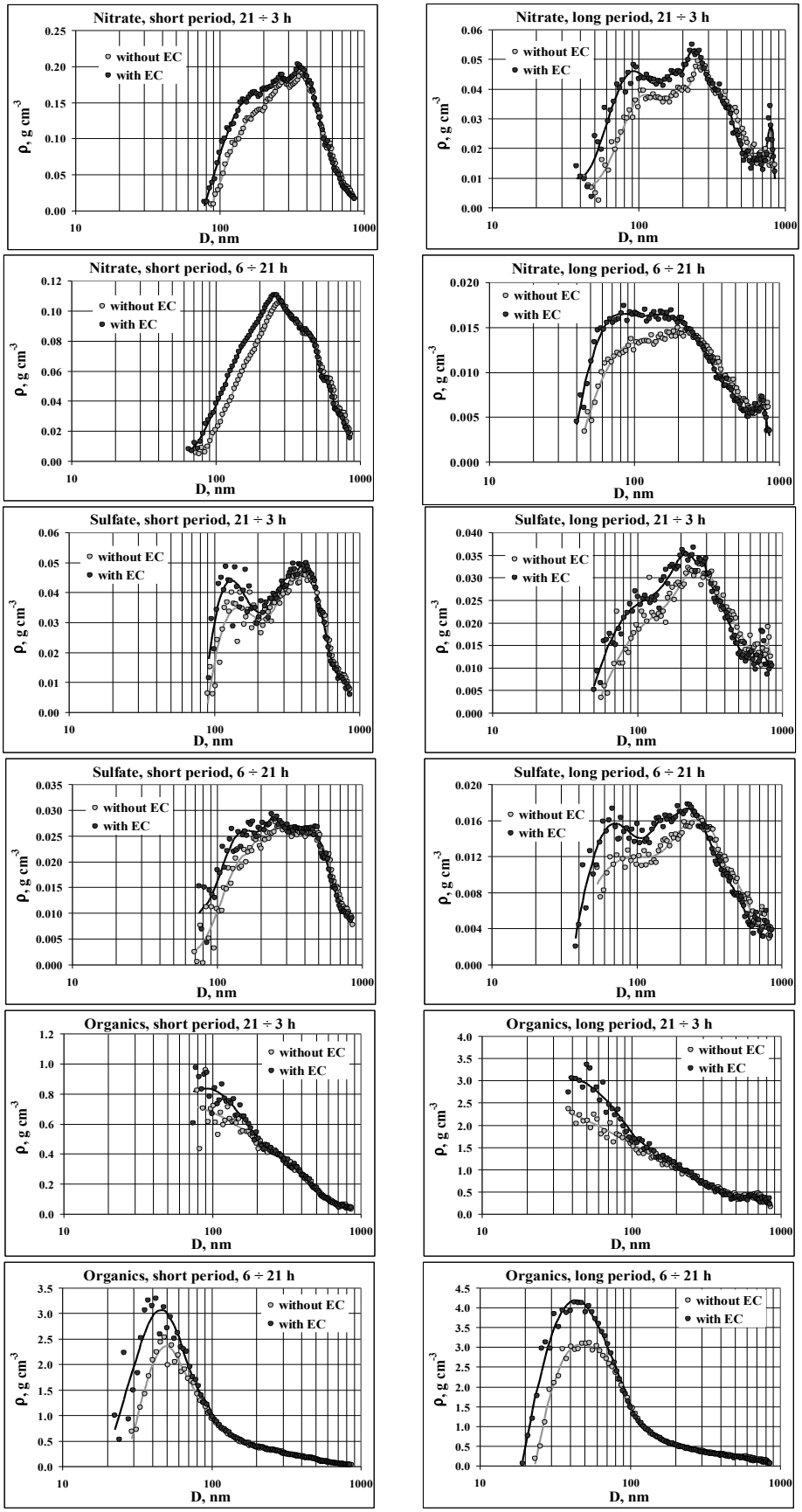

Fig. 3-10. Density spectra of chemical compounds in the aerosol particles including EC and not including EC.

Initially it was presumed that the density for the particles with the diameter above 100 nm should exceed 1 g cm^{-3}. The idea that Q-AMS and SMPS indicate the same particles in a different way was put forward: the mass of lower density particles is assigned to smaller particles, whereas SMPS captures the effective size. A few cases, when the Q-AMS registers aerosol particles as of the same size, but the SMPS system registers them as of different size, are presented in Fig. 3-11 a). A mass of a lower density particle mass determined with the Q-AMS is assigned to smaller particle when the SMPS system detects an effective particle size - larger than it is recorded with the Q-AMS. The density is calculated by dividing the weight by volume of the particles. Therefore, the quantity of small particulate matter with the Q-AMS will be increased and the quantity of major aerosol particles will be reduced. For this reason an increased organic density for particles with the diameter below 100 nm is obtained.

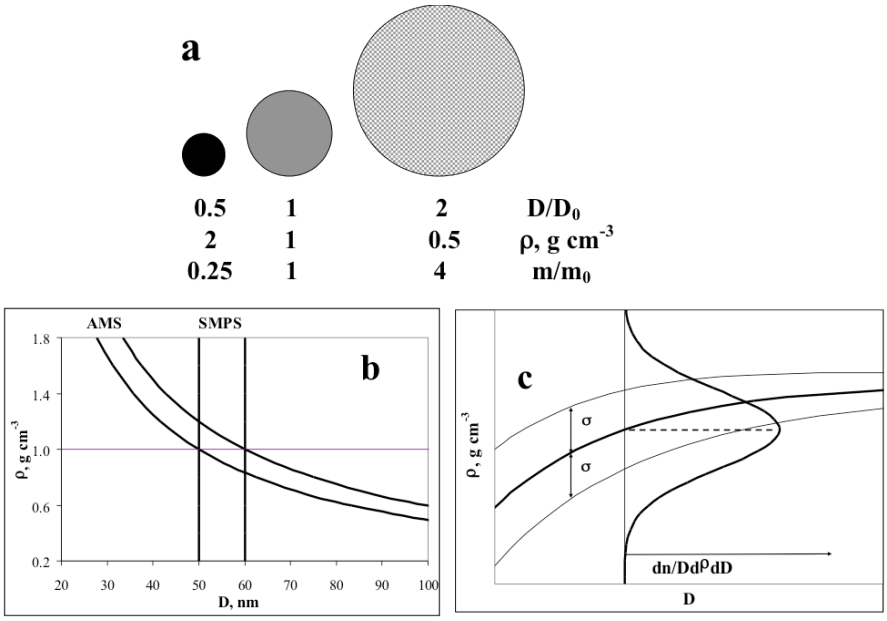

Fig. 3-11. (a) An example of how SMPS and Q-AMS indicate particles ($\rho D = const.$); (b) Q-AMS and SMPS measurement range in the size-density (ρ, D) graph; (c) Illustration of aerosol particles distribution in the (ρ, D) field.

3.2.2 The evaluation of organics matter density in aerosol particles with diameter below 100 nm

During the evaluation of the aerosol particle density the particles of the same size were considered to be homogeneous, i.e., all parts of the particle are of equal density. In general, aerosol particles of the same sizes are emitted from different sources, thus the material density in a particle set may vary. Distribution of water quantities in the aerosol particles by size is unknown. Furthermore, the particle of the same size can be either hydrophilic or hydrophobic. Particles can be of different densities during formation, especially fresh particles that are formed under the intensive influence of transport emission. Therefore, erroneous results on the evaluation of the particle density are derived when particles are considered to be homogeneous.

Fig. 3-11 b) shows how Q-AMS and SMPS will represent data for the particles in the range from 50 nm to 60 nm.

For further investigation the particles in the size range with the diameter below 100 nm (according to Q-AMS data) were selected. Particles in this range originate from the formation of traffic emission pollutants and are characterized by hydrophobic properties, dominated by an organic component, while there are no remaining chemical components or their amount is very little, i.e. they do not constitute a significant fraction. Therefore for detailed analysis diurnal hours of a long period were chosen, when the traffic is intensive, and the influence of sulfate and nitrate is minimal.

In order to analyze the influence of the EC contribution two cases were considered: i) all the mass of particles consists only of organics; ii) all the mass of particles consists of organics and EC. Modeling was carried out in the density-size graph field. It was presumed that all particles had a normal distribution (Fig. 3-11 c), where the median value of the aerosol particle density is:

$$\rho_m(D) = \rho_{m0}(1 - e^{-\alpha D}) \tag{3.9}$$

where ρ_{m0} and α are parameters of distribution.

The standard deviation:

$$\sigma_D = \sigma_0 e^{-\beta D} \tag{3.10}$$

where σ_0 and β are parameters of deviation.

The distribution is expressed by equation:

$$\frac{dn(\rho, D)}{d\rho dD} = \frac{dn_{SMPS}}{Dd\log D} e^{-\frac{(\rho-\rho_m(D))^2}{2\sigma_D^2}} \tag{3.11}$$

Using data obtained from SMPS ($\frac{dn_{SMPS}}{d\log D}$) mass of the particle for each diameter interval ($D_1 \div D_2$) with regard of condition $\rho D \approx const$ was derived:

$$M_{12} = \int_0^{\infty} \int_{\frac{\rho_0 D_1}{d}}^{\frac{\rho_0 D_2}{D}} \frac{\pi \rho D^3}{6} \cdot \frac{dn(\rho, D)}{d\rho dD} d\rho dD \tag{3.12}$$

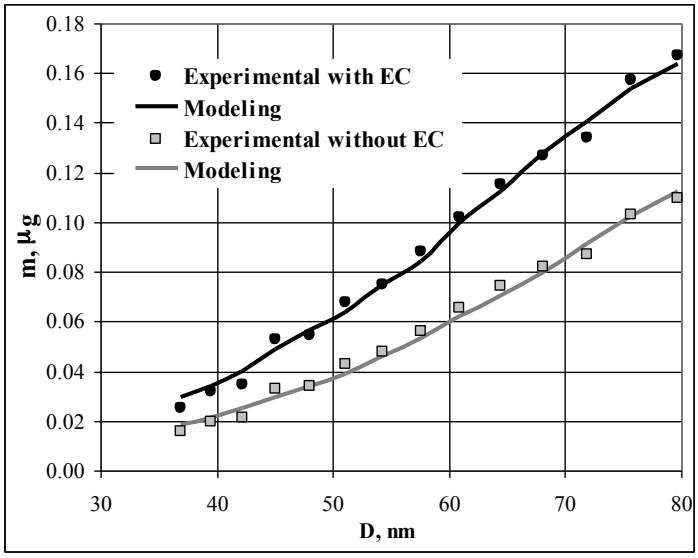

Fig. 3-12. Evaluation of organics mass concentration (experimental data – not including EC, modeling – including EC, literature data of EC used).

The derived mass was compared with data provided by the Q-AMS in the same range. By applying the least square method and varying parameters $\rho_{m0}, \alpha, \sigma_0, \beta$ a solution was found when theoretically derived and experimentally obtained values coincided (Fig. 3-12).

Table 3-3. Density and its standard deviation value of the particles with different diameters.

D, nm	**80**	**60**	**35**
without EC			
ρ	0.68	0.64	0.54
σ	0.061	0.090	0.149
with EC			
ρ	0.56	0.56	0.54
σ	0.010	0.014	0.024

The aerosol particle number distribution was modeled in (ρ, D) field. Results are presented in Fig. 3-13. It is seen that the density of the smallest particles is lower than 1 g cm^{-3}. Derived density distribution parameters (value of median density and standard deviation) for diameters 35 nm, 60 nm and 80 nm are given in Table 3-3. It is seen that the median value of the density decreases and the standard deviation is increasing with the decreasing diameter of the particles indicating that the emerging fresh particles formed aggregates. Q-AMS do not detect EC, therefore, the contribution of EC to measured PM1 was evaluated only theoretically based on literature data, thus the presented data with the EC contribution is extreme due to the used OC / EC ratio from the internal combustion engine.

Developed density evaluation method described herein 3.2.2 chapter (using lognormal distribution and starting with eq. 3.9) can be applied on the hydrophobic aerosol particles with diameter smaller than 100 nm for data simultaneously obtained with Q-AMS and SMPS. The drawback of this method is that EC contribution is evaluated only theoretically; hence to retrieve more accurate results data from EC measuring instrumentation should be included in calculations.

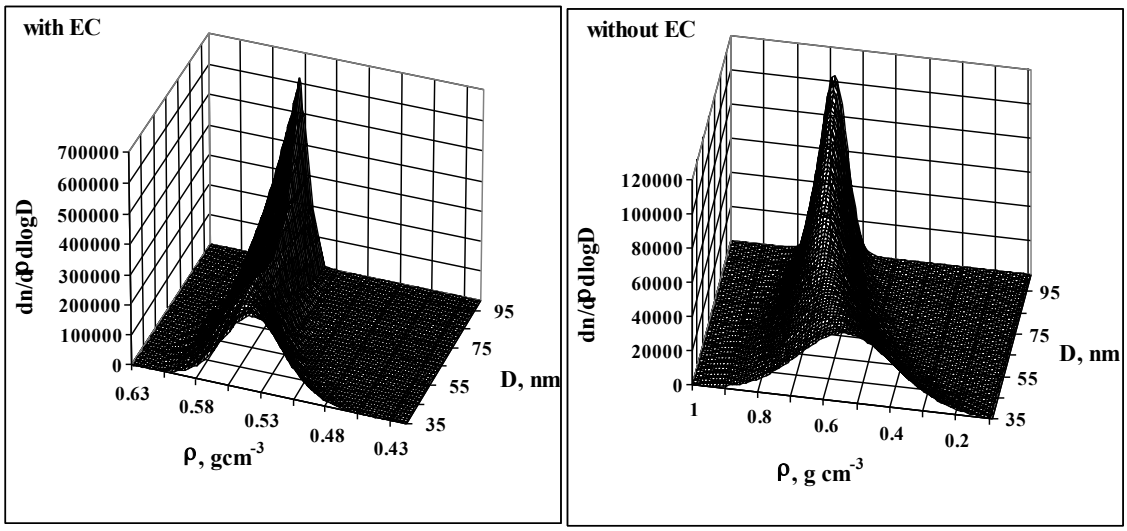

Fig. 3-13. Distribution of aerosol particle number concentration in ρ, *D* graph. Including EC (literature data used) and not including EC (experimental data).

However, it should be noted, that data are obtained only from one field measurement campaign under urban conditions during the spring period and analysis carried out by varying 4 parameters and applying a normal distribution of density for one mode. It means that results could be considered only as indicative and other studies employing EC measurement techniques should be carried out for example at the background sites to check the credibility of the method. Nevertheless, this analysis showed that modeling in (*ρ, D*) field enables evaluating particles material density for particles with diameter below 100 nm more accurately.

3.2.3 Conclusion

It is shown that in the urban environment during the intensive emission from transport newly formed atmospheric aerosol particles of the same size have a different density and tend to form aggregates.

It is obtained that the density of the smallest aerosol particles (< 100 nm) is less than 1 g cm^{-3} and the value of the median density decreases, whereas a

standard deviation of the density increases with the decreasing diameter of the aerosol particles.

For the data obtained by means of Q-AMS and SMPS set up it is recommended to model the particle size distribution in the size-density (ρ, D) field.

3.3 The extent of neutralization of acidic sulfates with atmospheric ammonia in volcanic origin PM1

Volcanoes emit a variety of gases and particles. Acidic sulfate aerosols are formed as a result of homogeneous and heterogeneous chemical reactions of sulfur dioxide in the atmosphere (Bao et al., 2010; von Glasow et al., 2009). Ammonia compounds interact with acidic sulfate aerosols in the atmosphere. Two concentration episodes of captured volcanic pollutants were selected for analysis to study the extent of particle neutralization: 0700-1400 UTC May 25 (Episode 1) and 0400-1100 UTC May 26 (Episode 2). The time series of hourly averaged concentrations of sulfate (SO_4^{2-}) and ammonium (NH_4^+) during the period of 25-26 May 2011 are analyzed in Fig. 3-14.

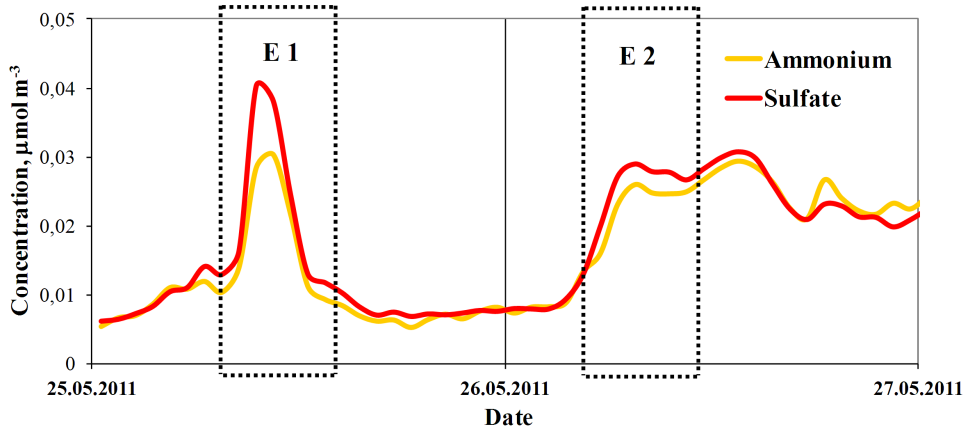

Fig. 3-14. Time series of hourly averaged concentrations of sulfate (SO_4^{2-}) and ammonium (NH_4^+) during the periods 0700-1400 UTC 25 May (Episode 1) and 0400-1100 UTC 26 May (Episode 2).

During Episode 1 the trajectory of air masses passed at a relatively high altitudes avoiding polluted industrial regions of Europe (see Fig. 3-15 a). Fig. 3-15 a) indicates that the air masses containing the volcanic pollutants descended to the surface from 3000-4000 m of troposphere. The dispersion of the plume (Episode 1) was very small over the Atlantic Ocean and a sharp increase of the sulfate and ammonium concentration was observed (Fig. 3-14). During Episode 2 the air masses trajectory passed at considerably lower altitudes and resulted in a mix of volcanic pollutants with previous volcanic emissions and pollutants of anthropogenic origin (see Fig. 3-15 b). The trajectory of air masses over the regions of Ireland, UK and Northern Germany passed over at relatively low altitudes. The higher altitude trajectory indicates air masses that arrived with pollutants emitted from the volcano eruption on May 23, 1800 H. These two episodes allowed us to compare and to evaluate neutralization peculiarities of acidic sulfates particles with ammonia in the atmosphere.

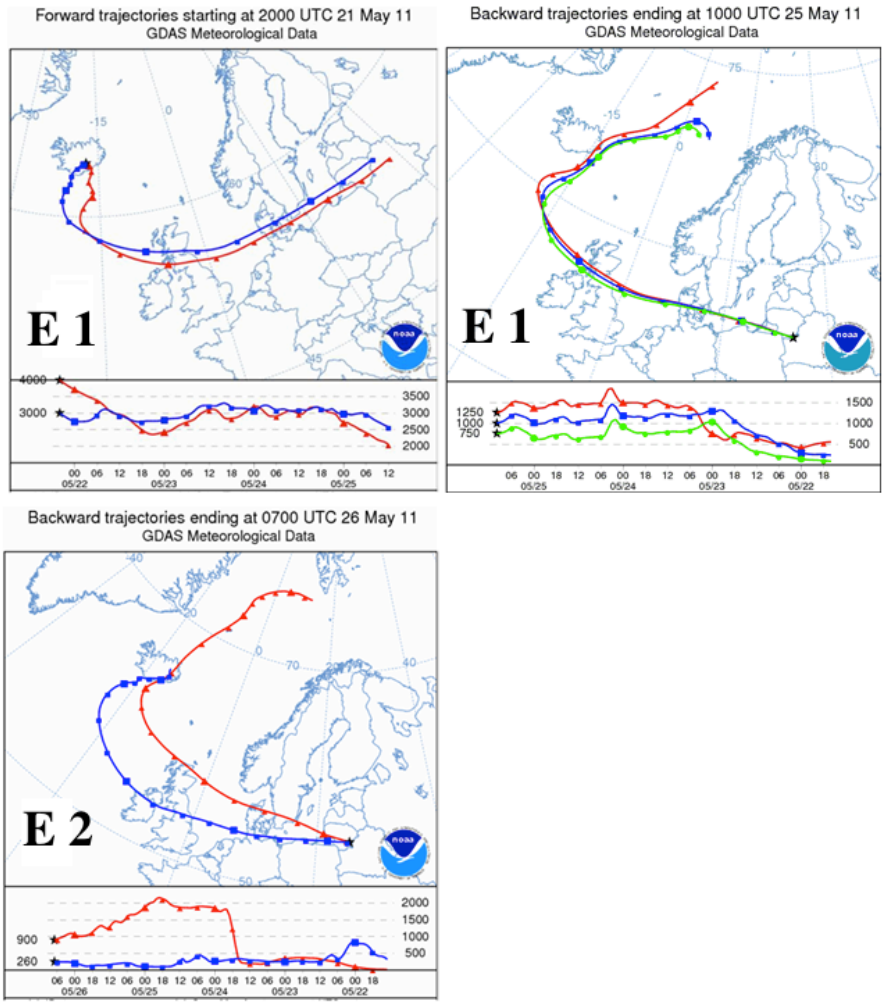

Fig. 3-15. Forward and backward trajectories of air masses during Episode 1 (a) and 2 (b).

Size-resolved molar distribution spectra of NH_4^+ and SO_4^{2-} molar concentrations during Episodes 1 and 2 are presented in Fig. 3-16. In both cases the distribution of concentrations is log-normal.

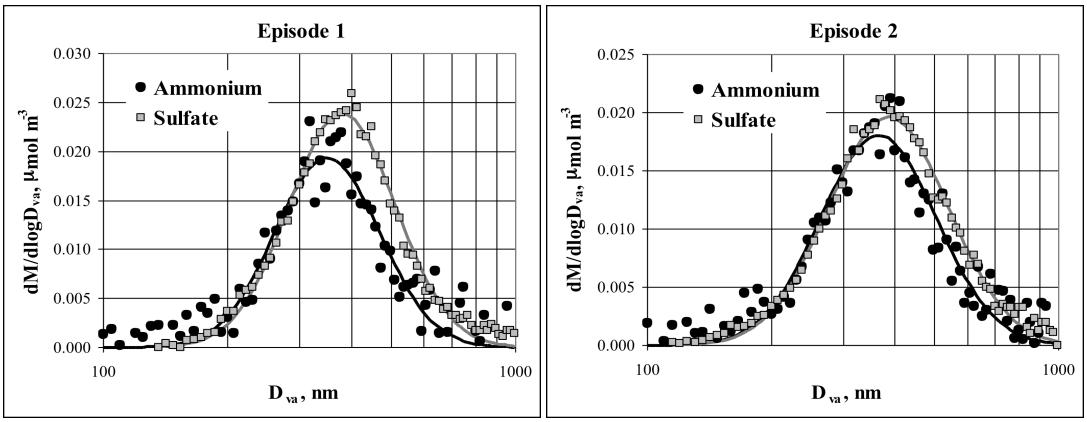

Fig. 3-16. Size-resolved distribution spectra of sulfate and ammonium molar concentrations during Episodes 1 and 2.

The Monte-Carlo method is applied in order to obtain a standard geometrical deviation of the median diameter. It is done in order to evaluate steadiness of the obtained distribution spectra of NH_4^+ and SO_4^{2-} molar concentrations during Episodes 1 and 2 (Fig. 3-16). Random numerical values of the new log-normal distribution corresponding to the average values and standard deviations of distribution spectra presented in Fig. 3-16 are generated. New obtained log-normal distribution yields new median values. Procedure is repeated 36 times. Obtained median values allow to evaluate standard geometrical deviation values of the simulated system. The extent of neutralization on the particle size of NH_4^+ and SO_4^{2-} is calculated. The neutralization extent of $(NH_4)_{2X}H_{2(1-X)}SO_4$ acidic sulfate particles (where the neutralization extent $X = M_{NH_4^+} / 2M_{SO_4^{2-}} \times 100\%$, $M_{NH_4^+}$ is the molar concentration of NH_4^+ and $M_{SO_4^{2-}}$ is the molar concentration of SO_4^{2-}) related to the aerosol particle size is depicted in Fig. 3-17. One can see that in the aerosol particles with diameter below 100 nm the acidic sulfates are fully neutralized with ammonia (the ratio is 1), whereas for larger particles the neutralization extent is declining.

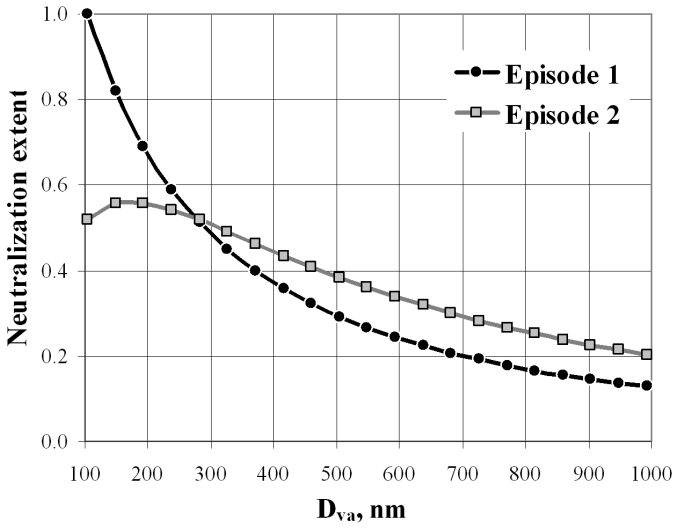

Fig. 3-17. Extent of acidic sulfate neutralization with ammonia related to the aerosol particle size during Episodes 1 and 2.

During Episode 2 the peaks of sulfate and ammonium are not as sharp as during Episode 1 and this is related with the very first eruption hours when emitted pollutants were relatively at high altitudes of the troposphere and reached the measurement site without any contact with industrial regions. The emitted pollutants (Episode 2) later got mixed with earlier emitted pollutants from the volcano and low altitude air masses contacted with the polluted air above industrial regions of Ireland, UK and northern Germany.

Data of Episode 1 enables us to make a rough estimation of the ammonia flux onto the aerosol particle surface. First of all it is rather crucial to analyze whether ammonia is deposited onto the surface of the particles during the transport with long-range air masses. For this reason the relation between the logarithmic volumetric median diameter value and the logarithmic surface area median diameter value was used. The difference between the logarithmic volumetric median diameter value and the logarithmic surface area median diameter value equals:

$$\ln D_{mV} - \ln D_{mS} = \ln^2 \sigma \qquad (3.13)$$

where D_{mV} is the volumetric median diameter distribution, D_{mS} is the surface area median diameter distribution, lnσ is the geometrical standard deviation.

Other expression:

$$D_{mV} = D_{mS} e^{\ln^2 \sigma} \_\_ or \_\_ D_{mS} = D_{mV} e^{-\ln^2 \sigma} \qquad (3.14)$$

The estimation of log-normal distribution of the median diameter magnitude and its error estimation was performed by applying the Monte Carlo method. Median diameter value of lognormal distribution of ammonium and sulfate concentrations in aerosol particles and values obtained using (3.14) are presented in Table 3-4.

Table 3-4. Median diameter value of lognormal distribution of NH_4^+ and SO_4^{2-} concentrations and their standard deviations during Episodes 1 and 2.

NH_4^+		SO_4^{2-}	
D_m, nm	$D_m e^{\ln^2 \sigma_{NH_4^+}}$, nm	D_m, nm	$D_m e^{-\ln^2 \sigma_{SO_4^{2-}}}$, nm
Episode 1			
349.0 ± 3.4	381.0 ± 4.6	379.6 ± 1.2	346.7 ± 1.3
Episode 2			
364.3 ± 3.1	404.8 ± 4.2	385.3 ± 1.4	343.9 ± 1.5

From Table 3-4. it is seen that during Episode 1 the corrected median diameter value of ammonium-containing particles (within the limits of error) very well coincides with the median diameter value of sulfate-containing particles (381.0 ± 4.6 nm and 379.6 ± 1.2 nm) and on the contrary, the corrected median diameter value of sulfate-containing particles (within the limits of error) is consistent with the median diameter value of ammonium-

containing particles (346.7 ± 1.3 nm and 349.0 ± 3.4 nm). Thus, it indicates that NH_4^+ and SO_4^{2-} containing aerosol particles are of the same origin, having the same lognormal distribution diameter number and this also indicates that ammonia is deposited on the surface area of the sulfate-containing aerosol particles during transfer with the air masses to the measurement site. Similar coincidence of median diameter values is not observed in Episode 2 because air masses from this episode were mixed with older air masses.

Finally, a rough estimation of the ammonia flux onto the aerosol particle surface has been made using data of Episode 1. During this episode the average NH_4^+ concentration was 0.83 μg m^{-3} and that of SO_4^{2-} – 6.02 μg m^{-3}. The influence of nitrates was neglected due to the low mass (0.5 %) compared with the mass of all chemical components. The mass of elemental carbon (EC) made up 20 % of the organic carbon mass (OC) (Gan et al., 2011; Turpin and Lim, 2001; Xing et al., 2013). Based on data of the study of Mohr et al. (2012) it has been accepted that the density of ammonium is 1.75 g cm^{-3}, that of sulfate – 1.78 g cm^{-3}, that of organics –1.5 g cm^{-3}, that of EC – 1.77 g cm^{-3} (Zhang et al., 2005) and that of water is 1.0 g cm^{-3}. The water mass was calculated by evaluation of the aerosol particle growing factor due to humidity. When the humidity is close to 50 % ÷ 60 % and the temperature is about 12^0C ÷ 15^0C, the aerosol particle growth factor, based on literature data, is from 1.2 to 1.5 (Michel Flores et al., 2012). Using above data, the resultant aerosol particle densities were evaluated:

$$\rho(D_{va}) = \frac{\sum_{i=1}^{n} m_i(D_{va})}{\sum_{i=1}^{n} \frac{m_i(D_{va})}{\rho_{0i}}} \tag{3.15}$$

$m_i(D_{va})$ is the mass of the aerosol particle chemical component *i* with the diameter D_{va}, ρ_{0i} is the density of the chemical component *i*.

Based on the calculated densities the diameters of aerosol particles have been corrected:

$$D = \frac{\rho_0}{\rho(D_{va})} D_{va} \tag{3.16}$$

ρ_0 is the water density.

Values from Q-AMS, $\frac{dm_i(D_{va})}{d\log D_{va}}$ have been corrected based on corrected diameters:

$$\frac{dm_i(D)}{d\ln D} = \frac{1}{\ln(10)} \cdot \frac{dm_i(D_{va})}{d\log D_{va}} \cdot \frac{\Delta\ln D_{va}}{\Delta\ln D} \tag{3.17}$$

Aerosol particle masses were calculated:

$$m(D) = \frac{1}{6}\rho(D)\pi D^3 \tag{3.18}$$

The size resolved particle number distribution in regard to their diameter was calculated:

$$\frac{dn}{d\ln D} = \frac{1}{m(D)} \sum_{i=1}^{n} \frac{dm_i(D)}{d\ln D} \tag{3.19}$$

The particle surface area is equal to $s = \pi D^2$, then:

$$\frac{dS}{d\ln D} = \pi D^2 \frac{dn}{d\ln D} \tag{3.20}$$

The whole particle surface area in the mode is equal to:

$$S = \int_{D_1}^{D_2} \frac{dS}{D d\ln D} dD \tag{3.21}$$

By dividing the NH_4^+ amount in the mode m_{am} to the surface area S of all particles in the mode and time T during which aerosol particles were transported with air masses to the measurement point, we obtain the value of NH_4^+ flux to the particle surface area:

$$\frac{dm}{dSdt} = \frac{m_{am}}{ST} \cdot \frac{\mu_{NH_3}}{\mu_{NH4^+}} \tag{3.22}$$

where μ_{NH_3} is moles of ammonia, $\mu_{NH_4^+}$ is moles of ammonium. The duration of aerosol particles being advected with the air masses to the measurement point is 86 ± 4 hours. According to these data the NH_4^+ flux to the particle surface area has been evaluated to be from 30 μg m^{-2} h^{-1} to 55 μg m^{-2} h^{-1} (if assumed that particles all the time were dry, the flux would be 74 μg m^{-2} h^{-1}). The above presented average values are approximate because the meteorological conditions during transport of air masses were unknown. Probably the highest flux was when aerosol particles were transported at the lowest atmospheric height. Thus, the flux value in this case would be higher. Expected lifetime for aerosol particles in the atmosphere with the diameter below 1 μm is on the average 7 days (Jeanicke, 1980). This implies that the volcanic origin acidic sulfate particle neutralization with ammonia is also partial and that the acidic particles of volcanic origin favor the formation of acidic precipitation.

3.3.1 Conclusion

Acidic sulfates on volcanic origin aerosol particles can be fully neutralized with atmospheric ammonia when their size is of about tenths of nanometers, whereas the larger particles have a lower extent of neutralization. Therefore, the neutralization of acidic sulfates with ammonia in volcanic origin aerosol particles can be estimated only based on the size of aerosol particles. Volcanic origin aerosol particles favor the formation of acidic precipitation.

The atmospheric ammonia flux to the aerosol particle surface area, depending on meteorological conditions, can vary approximately from 30 to 74 μg m^{-2} h^{-1}.

4 THE MAIN CONLUSIONS

1. Organics accounts from 68.8 % to 77.1 % of the measured volatile and semi-volatile non-refractory compounds in submicron particle mass concentration at the background and urban sites in Lithuania during a mild season.
2. Hydrocarbon-like organic aerosols (HOA, 28 %), biomass burning organic aerosols (BBOA, 32 %) and semi-volatile organic aerosols (SV-OOA, 40 %) are the main sources of organics at the Vilnius site; BBOA (32 %), SV-OOA (47 %) and LV-OOA (21 %) are identified to be the main sources of organics at the Rūgšteliškis site (background site); LV-OOA (64 %) and SV-OOA (36 %) are identified at the Preila (coastal/marine) site. Organic aerosols of SV-OOA factor are more oxygenated at the background sites if compared to organic aerosols of SV-OOA factor at urban site.
3. Analysis indicated that ammonium nitrate mass concentration (61 ± 9 %, 61 ± 5 %, 80 ± 3 % respectively at Vilnius, Rūgšteliškis, Preila) made a greater contribution than that of ammonium sulfate (37 ± 5 %, 44 ± 2 %, 36 ± 2 % respectively Vilnius, Rūgšteliškis, and Preila sites) to that of the total of ammonium during a mild season.
4. Particles (with diameter below 100 nm) tend to form aggregates and have different effective matter density less than 1 g cm^{-3} at an urban site during formation under the influence of intensive transport emission. Particles number distribution modeling in the density – size (ρ, D) diagram allows estimating matter density of the particles more accurately.
5. Acidic sulfates on volcanic origin aerosol particles tend to be fully neutralized with atmospheric ammonia when their size is of about tenths of nanometers, whereas the larger particles have a lower extent of neutralization in long-range transport air masses advected to Lithuania.

ACKNOWLEDGEMENT

I am profoundly grateful to the scientific supervisor dr. Kęstutis Kvietkus (State research institute Center for Physical Sciences and Technology) for the patient scientific guidance and unwavering support along with invaluable discussions throughout the years of the study and during the preparation of this thesis. This thesis would not be accomplished without encouraging support. I am truly fortunate to have the opportunity to continue my journey through the science of atmospheric aerosols at the laboratory of Atmospheric Pollution Research since the third year of my bachelor studies.

Special words of sincere gratitude are acknowledged to dr. Jonas Šakalys (State research institute Center for Physical Sciences and Technology, laboratory of Atmospheric Pollution Research) for his valuable insights, advices and lessons. Without his valuable contribution this work would be immeasurably more difficult.

I also would like to take this opportunity and say thank you to Prof. habil. dr. Algimantas Undzėnas (State research institute Center for Physical Sciences and Technology) for valuable insights on the 3rd part of this dissertation. Dr. Vidmantas Ulevičius (State research institute Center for Physical Sciences and Technology) for the opportunity to use SMPS data. I am also grateful to dr. Lina Davulienė for useful remarks on the preparation of the manuscript. I greatly appreciate remarks and advices from the colleagues of Department of Environmental Research during seminars.

Finally, I would like to say thank You to my beloved relatives for unconditional support and assistance when needed and of course to my dearest husband who was the one I can always rely on.

5 REFERENCES

Adame, J.A., Valentí – Pía, M.D., Gil-Ojeda, M., 2015. Impact evaluation of potential volcanic plumes over Spain. Atmos. Res. 160, 39–49. doi:10.1016/j.atmosres.2015.03.002

Bao, H., Yu, S., Tong, D.Q., 2010. Massive volcanic SO(2) oxidation and sulphate aerosol deposition in Cenozoic North America. Nature 465, 909–912. doi:10.1038/nature09100

Baustian, K.J., Wise, M.E., Tolbert, M.A., 2010. Depositional ice nucleation on solid ammonium sulfate and glutaric acid particles. Atmos. Chem. Phys. 10, 2307–2317.

Behera, S.N., Sharma, M., Aneja, V.P., Balasubramanian, R., 2013. Ammonia in the atmosphere: A review on emission sources, atmospheric chemistry and deposition on terrestrial bodies. Environ. Sci. Pollut. Res. 20, 8092–8131. doi:10.1007/s11356-013-2051-9

Bell, M.L., Davis, D.L., Fletcher, T., 2008. A retrospective assessment of mortality from the london smog episode of 1952: The role of influenza and pollution. Urban Ecol. An Int. Perspect. Interact. Between Humans Nat. 112, 263–268. doi:10.1007/978-0-387-73412-5_15

Biskos, G., Buseck, P.R., Martin, S.T., 2009. Hygroscopic growth of nucleation-mode acidic sulfate particles. J. Aerosol Sci. 40, 338–347. doi:10.1016/j.jaerosci.2008.12.003

Brus, D., Neitola, K., Hyvärinen, a.-P., Petäjä, T., Vanhanen, J., Sipilä, M., Paasonen, P., Kulmala, M., Lihavainen, H., 2011. Homogenous nucleation of sulfuric acid and water at close to atmospherically relevant conditions. Atmos. Chem. Phys. 11, 5277–5287. doi:10.5194/acp-11-5277-2011

Canagaratna, M.R., Jayne, J.T.J.T., Jimenez, J.L., Allan, J.D., Alfarra, M.R., Zhang, Q.Q., Onasch, T.B., Drewnick, F., Coe, H., Middlebrook, A.M., Delia, A., Williams, L.R., Trimborn, A.M., Northway, M.J., DeCarlo, P.F., Kolb, C.E., Davidovits, P., Worsnop, D.R., 2007. Chemical and microphysical characterization of ambient aerosols with the Aerodyne Aerosol Mass Spectrometer. Mass Spectrom. Rev. 26, 185–222. doi:10.1002/mas

Chien, S.M., Huang, Y.J., Chuang, S.C., Yang, H.H., 2009. Effects of biodiesel blending on particulate and polycyclic aromatic hydrocarbon emissions in

Nano/Ultrafine/Fine/Coarse ranges from diesel engine. Aerosol Air Qual. Res. 9, 18–31. doi:10.4209/aaqr.2008.09.0040

Chio, C.P., Liao, C.M., 2008. Assessment of atmospheric ultrafine carbon particle-induced human health risk based on surface area dosimetry. Atmos. Environ. 42, 8575–8584. doi:10.1016/j.atmosenv.2008.08.027

Dall'Osto, M., Harrison, R.M., 2012. Urban organic aerosols measured by single particle mass spectrometry in the megacity of London. Atmos. Chem. Phys. 12, 4127–4142. doi:10.5194/acp-12-4127-2012

Dall'Osto, M., Harrison, R.M., Beddows, D.C.S., Freney, E.J., Heal, M.R., Donovan, R.J., 2006. Single-particle detection efficiencies of aerosol time-of-flight mass spectrometry during the North Atlantic marine boundary layer experiment. Environ. Sci. Technol. 40, 5029–35. doi:10.1021/es050951i

DeCarlo, P., Slowik, J., 2004. Particle morphology and density characterization by combined mobility and aerodynamic diameter measurements. Part 1: Theory. Aerosol Sci. … 38, 1185–1205. doi:10.1080/027868290903907

Dockery, D.W., Pope, C. a, 1994. Acute respiratory effects of particulate air pollution. Annu. Rev. Public Health 15, 107–132. doi:10.1146/annurev.pu.15.050194.000543

Dominici, F., Peng, R.D., Bell, M.L., Pham, L., McDermott, A., Zeger, S.L., Samet, J.M., 2006. Fine particulate air pollution and hospital admission for cardiovascular and respiratory diseases. JAMA 295, 1127–1134. doi:10.1001/jama.295.10.1127

Draxler, R.R., Rolph, G.D., 2014. HYSPLIT (HYbrid Single-Particle Lagrangian Integrated Trajectory) Model access via NOAA ARL READY Website (http://www.arl.noaa.gov/HYSPLIT.php). NOAA Air Resources Laboratory, College Park, MD. NOAA Air Resour. Lab.

Du, H.H., Kong, L.D., Cheng, T.T., Cheng, J.M., Yang, X., Zhang, R.Y., Han, Z.W., Yan, Z., Ma, Y.L., 2010. Insights into ammonium particle-to-gas conversion: non-sulfate ammonium coupling with nitrate and chloride. Aerosol Air Qual. Res. 10, 589–595.

Ehn, M., Petäjä, T., Aufmhoff, H., Aalto, P., Hämeri, K., Arnold, F., Laaksonen, a., Kulmala, M., 2006. Hygroscopic properties of ultrafine aerosol particles in the boreal forest: diurnal variation, solubility and the

influence of sulfuric acid. Atmos. Chem. Phys. Discuss. 6, 9937–9965. doi:10.5194/acpd-6-9937-2006

Finessi, E., Decesari, S., Paglione, M., Giulianelli, L., Carbone, C., Gilardoni, S., Fuzzi, S., Saarikoski, S., Raatikainen, T., Hillamo, R., Allan, J., Mentel, T.F., Tiitta, P., Laaksonen, a., Petäjä, T., Kulmala, M., Worsnop, D.R., Facchini, M.C., 2012. Determination of the biogenic secondary organic aerosol fraction in the boreal forest by NMR spectroscopy. Atmos. Chem. Phys. 12, 941–959. doi:10.5194/acp-12-941-2012

Fisher, J.A., Jacob, D.J., Wang, Q., Bahreini, R., Carouge, C.C., Cubison, M.J., Dibb, J.E., Diehl, T., Jimenez, J.L., Leibensperger, E.M., Lu, Z., Meinders, M.B.J., Pye, H.O.T., Quinn, P.K., Sharma, S., Streets, D.G., Donkelaar, A. Van, Yantosca, R.M., 2011. Author ' s personal copy Sources , distribution , and acidity of sulfate e ammonium aerosol in the Arctic in winter e spring Author ' s personal copy. Atmos. Environ. 45, 7301–7318. doi:10.1016/j.atmosenv.2011.08.030

Gan, T.H., Hield, P., Boere, B., Bentley, M., Cogdon, T., Hanhela, P.J., Anderson, B., Gillett, R., 2011. Field Characterisation of Diesel Particulate Emissions From a Euro 0 Engine, in: 15th ETH-Conference on Combustion Generated Nanoparticles Zurich, Switzerland.

Gantt, B., Meskhidze, N., Facchini, M.C., Rinaldi, M., Ceburnis, D., O'Dowd, C.D., 2011. Wind speed dependent size-resolved parameterization for the organic mass fraction of sea spray aerosol. Atmos. Chem. Phys. 11, 8777–8790. doi:10.5194/acp-11-8777-2011

Garbariene, I., Kvietkus, K., Šakalys, J., Ovadnevaitė, J., Čeburnis, D., 2012. Biogenic and anthropogenic organic matter in aerosol over continental Europe: source characterization in the east Baltic region. J. Atmos. Chem. 69, 159–174. doi:10.1007/s10874-012-9232-7

Goldstein, A.H., Worton, D.R., Williams, B.J., Hering, S. V, Kreisberg, N.M., Panić, O., Górecki, T., 2008. Thermal desorption comprehensive two-dimensional gas chromatography for in-situ measurements of organic aerosols. J. Chromatogr. A 1186, 340–7. doi:10.1016/j.chroma.2007.09.094

Guarieiro, L.L.N., Guarieiro, A.L.N., 2013. Vehicle Emissions : What Will Change with Use of Biofuel ?, in: Biofuels - Economy, Environment and Sustainability. doi:10.5772/52513

Guffanti, M., Casadevall, T.J., Budding, K., 2009. Encounters of aircraft with volcanic ash clouds; a compilation of known incidents 1953-2009 [WWW Document]. U.S. Geol. Surv. Data Ser. 545, ver. 10, Plus 4 Append. Incl. Compil. Database. URL http://pubs.usgs.gov/ds/545

Hallquist, M., Wenger, J.C., Baltensperger, U., Rudich, Y., Simpson, D., Claeys, M., Dommen, J., Donahue, N.M., George, C., Goldstein, a. H., Hamilton, J.F., Herrmann, H., Hoffmann, T., Iinuma, Y., Jang, M., Jenkin, M.E., Jimenez, J.L., Kiendler-Scharr, a., Maenhaut, W., McFiggans, G., Mentel, T.F., Monod, a., Prévôt, a. S.H., Seinfeld, J.H., Surratt, J.D., Szmigielski, R., Wildt, J., 2009. The formation, properties and impact of secondary organic aerosol: current and emerging issues. Atmos. Chem. Phys. 9, 5155–5236. doi:10.5194/acp-9-5155-2009

Halmer, M.M., Schmincke, H.U., Graf, H.F., 2002. The annual volcanic gas input into the atmosphere, in particular into the stratosphere: A global data set for the past 100 years. J. Volcanol. Geotherm. Res. 115, 511–528. doi:10.1016/S0377-0273(01)00318-3

Hanel, G., Thudium, J., 1977. Mean Bulk Densities of Samples of Dry Atmospheric Aerosol Particles – Summary of Measured Data. Pure Appl. Geophys. 115, 799–803.

Harrison, R.M., 1999. Understanding Our Environment: An Introduction to Environmental Chemistry and Pollution. Cambridge, UK: The Royal Society of Chemistry.

Hennigan, C.J., Bergin, M.H., Dibb, J.E., Weber, R.J., 2008. Enhanced secondary organic aerosol formation due to water uptake by fine particles. Geophys. Res. Lett. 35, L18801. doi:L18801\r10.1029/2008gl035046

Hinds, W.C., 2012. Aerosol technology: properties, behavior, and measurement of airborne particles, New York, Wiley-Interscience, 1982. 442 p. doi:10.1017/CBO9781107415324.004

Hu, M., Peng, J., Sun, K., Yue, D., Guo, S., Wiedensohler, A., Wu, Z., 2012. Estimation of size--resolved ambient particle density based on the measurement of aerosol number, mass, and chemical size distributions in the winter in Beijing. Environ. Sci. Technol. 46, 9941–7. doi:10.1021/es204073t

IPCC, 2013. IPCC, 2013: Summary for Policymakers., in: Climate Change

2013: The Physical Science Basis. Contribution of Working Group I to the Fifth Assessment Report of the Intergovernmental Panel on Climate Change. pp. 1–28.

IPCC, I.P.C.C., 2007. IPCC, 2007: Summary for Policymakers, in Solomon, S., D. Qin, M. Manning, Z. Chen, M. Marqu eds. The Physical Science Basis. Contribution of Working Group I to the Fourth Assessment Report of the Intergovernmental Panel on Climate Change. doi:10.2134/jeq2008.0015br

Jayne, J.T., Leard, D.C., Zhang, X., Davidovits, P., Smith, K.A., Kolb, C.E., Worsnop, D.R., 2000. Development of an Aerosol Mass Spectrometer for Size and Composition Analysis of Submicron Particles. Aerosol Sci. Technol. 33, 49–70. doi:10.1080/027868200410840

Jeanicke, R., 1980. Atmospheric aerosols and global climate. J. Aerosol Sci 11, 577–588.

Jimenez, J.L., 2003. Ambient aerosol sampling using the Aerodyne Aerosol Mass Spectrometer. J. Geophys. Res. 108, 1–13. doi:10.1029/2001JD001213

Jimenez, J.L., Canagaratna, M.R., Donahue, N.M., Prevot, A.S.H., Zhang, Q., Kroll, J.H., DeCarlo, P.F., Allan, J.D., Coe, H., Ng, N.L., Aiken, A.C., Docherty, K.S., Ulbrich, I.M., Grieshop, A.P., Robinson, A.L., Duplissy, J., Smith, J.D., Wilson, K.R., Lanz, V.A., Hueglin, C., Sun, Y.L., Tian, J., Laaksonen, A., Raatikainen, T., Rautiainen, J., Vaattovaara, P., Ehn, M., Kulmala, M., Tomlinson, J.M., Collins, D.R., Cubison, M.J., Dunlea, J., Huffman, J.A., Onasch, T.B., Alfarra, M.R., Williams, P.I., Bower, K., Kondo, Y., Schneider, J., Drewnick, F., Borrmann, S., Weimer, S., Demerjian, K., Salcedo, D., Cottrell, L., Griffin, R., Takami, A., Miyoshi, T., Hatakeyama, S., Shimono, A., Sun, J.Y., Zhang, Y.M., Dzepina, K., Kimmel, J.R., Sueper, D., Jayne, J.T., Herndon, S.C., Trimborn, A.M., Williams, L.R., Wood, E.C., Middlebrook, A.M., Kolb, C.E., Baltensperger, U., Worsnop, D.R., 2009. Evolution of Organic Aerosols in the Atmosphere. Science (80-.). 326, 1525–1529. doi:10.1126/science.1180353

Kanakidou, M., Seinfeld, J.H., Pandis, S.N., Barnes, I., Dentener, F.J., Facchini, M.C., Van Dingenen, R., Ervens, B., Nenes, A., Nielsen, C.J., Swietlicki, E., Putaud, J.P., Balkanski, Y., Fuzzi, S., Horth, J., Moortgat,

G.K., Winterhalter, R., Myhre, C.E.L., Tsigaridis, K., Vignati, E., Stephanou, E.G., Wilson, J., 2005. Organic aerosol and global climate modelling: a review. Atmos. Chem. Phys. 5, 1053–1123. doi:10.5194/acp-5-1053-2005

Kannosto, J., Lemmetty, M., Virtanen, a., Mäkelä, J.M., Keskinen, J., Junninen, H., Hussein, T., Aalto, P., Kulmala, M., 2008. Mode resolved density of atmospheric aerosol particles. Atmos. Chem. Phys. Discuss. 8, 7263–7288. doi:10.5194/acpd-8-7263-2008

Kerminen, V.M., Niemi, J. V., Timonen, H., Aurela, M., Frey, A., Carbone, S., Saarikoski, S., Teinilä, K., Hakkarainen, J., Tamminen, J., Vira, J., Prank, M., Sofiev, M., Hillamo, R., 2011. Characterization of a volcanic ash episode in southern Finland caused by the Grimsvötn eruption in Iceland in May 2011. Atmos. Chem. Phys. 11, 12227–12239. doi:10.5194/acp-11-12227-2011

Kirkby, J., Curtius, J., Almeida, J., Dunne, E., Duplissy, J., Ehrhart, S., Franchin, A., Gagné, S., Ickes, L., Kürten, A., Kupc, A., Metzger, A., Riccobono, F., Rondo, L., Schobesberger, S., Tsagkogeorgas, G., Wimmer, D., Amorim, A., Bianchi, F., Breitenlechner, M., David, A., Dommen, J., Downard, A., Ehn, M., Flagan, R.C., Haider, S., Hansel, A., Hauser, D., Jud, W., Junninen, H., Kreissl, F., Kvashin, A., Laaksonen, A., Lehtipalo, K., Lima, J., Lovejoy, E.R., Makhmutov, V., Mathot, S., Mikkilä, J., Minginette, P., Mogo, S., Nieminen, T., Onnela, A., Pereira, P., Petäjä, T., Schnitzhofer, R., Seinfeld, J.H., Sipilä, M., Stozhkov, Y., Stratmann, F., Tomé, A., Vanhanen, J., Viisanen, Y., Vrtala, A., Wagner, P.E., Walther, H., Weingartner, E., Wex, H., Winkler, P.M., Carslaw, K.S., Worsnop, D.R., Baltensperger, U., Kulmala, M., 2011. Role of sulphuric acid, ammonia and galactic cosmic rays in atmospheric aerosol nucleation. Nature 476, 429–433. doi:10.1038/nature10343

Kulmala, M., Laakso, L., Lehtinen, K.E.J., Riipinen, I., Dal Maso, M., Anttila, T., Kerminen, V.-M., Hõrrak, U., Vana, M., Tammet, H., 2004. Initial steps of aerosol growth. Atmos. Chem. Phys. Discuss. 4, 2553–2560. doi:10.5194/acpd-4-5433-2004

Kulmala, M., Lehtinen, K.E.J., Laaksonen, a., 2006. Cluster activation theory as an explanation of the linear dependence between formation rate of 3nm particles and sulphuric acid concentration. Atmos. Chem. Phys. 6, 787–793. doi:10.5194/acp-6-787-2006

Kvietkus, K., Šakalys, J., Didžbalis, J., Garbariene, I., Špirkauskaite, N., Remeikis, V., 2013. Atmospheric aerosol episodes over Lithuania after the May 2011 volcano eruption at Grimsvötn, Iceland. Atmos. Res. 122, 93–101. doi:10.1016/j.atmosres.2012.10.014

Kvietkus, K., Šakalys, J., Rimšelytė, I., Ovadnevaitė, J., Remeikis, V., Špakauskas, V., 2011. Characterization of aerosol sources at urban and background sites in Lithuania. Lith. J. Phys. 51, 65–74. doi:10.3952/lithjphys.51106

Li, X.Y., Gilmour, P.S., Donaldson, K., MacNee, W., 1996. Free radical activity and pro-inflammatory effects of particulate air pollution (PM10) in vivo and in vitro. Thorax 51, 1216–22. doi:10.1136/thx.51.12.1216

Liggio, J., Li, S.-M., Vlasenko, A., Stroud, C., Makar, P., 2011. Depression of ammonia uptake to sulfuric acid aerosols by competing uptake of ambient organic gases. Environ. Sci. Technol. 45, 2790–6. doi:10.1021/es103801g

Lin, Y., Wu, Y.G., Chang, C.-T., 2007. Combustion characteristics of waste-oil produced biodiesel/diesel fuel blends. Fuel 86, 1772–1780. doi:10.1016/j.fuel.2007.01.012

Liu, P., Ziemann, P.J., Kittelson, D.B., McMurry, P.H., 1995. Generating Particle Beams of Controlled Dimensions and Divergence: II. Experimental Evaluation of Particle Motion in Aerodynamic Lenses and Nozzle Expansions. Aerosol Sci. Technol. 22, 314–324. doi:10.1080/02786829408959749

Lohmann, U., Feichter, J., 2004. Global indirect aerosol effects: a review. Atmos. Chem. Phys. Discuss. 4, 7561–7614. doi:10.5194/acpd-4-7561-2004

Malloy, Q.G.J., Nakao, S., Qi, L., Austin, R., Stothers, C., Hagino, H., Cocker, D.R., 2009. Real-Time Aerosol Density Determination Utilizing a Modified Scanning Mobility Particle Sizer—Aerosol Particle Mass Analyzer System. Aerosol Sci. Technol. 43, 673–678. doi:10.1080/02786820902832960

Martin, S.T., Hung, H.-M., Park, R.J., Jacob, D.J., Spurr, R.J.D., Chance, K. V., Chin, V., 2004. Effects of the physical state of tropospheric ammonium-sulfate-nitrate particles on global aerosol direct radiative forcing. Atmos. Chem. Phys. 4, 183–214. doi:10.5194/acpd-3-5399-2003

Mcmurry, P.H., Takano, H., Anderson, G.R., 1983. Study of the ammonia (gas) – sulfuric acid (aerosols) reaction rate. Environ. Sci. Technol. 17.

McMurry, P.H., Wang, X., Park, K., Ehara, K., 2002. The Relationship between Mass and Mobility for Atmospheric Particles: A New Technique for Measuring Particle Density. Aerosol Sci. Technol. 36, 227–238. doi:10.1080/027868202753504083

Mensah, a. a., Holzinger, R., Otjes, R., Trimborn, a., Mentel, T.F., Ten Brink, H., Henzing, B., Kiendler-Scharr, a., 2012. Aerosol chemical composition at Cabauw, the Netherlands as observed in two intensive periods in May 2008 and March 2009. Atmos. Chem. Phys. 12, 4723–4742. doi:10.5194/acp-12-4723-2012

Merikanto, J., Napari, I., Vehkamäki, H., Anttila, T., Kulmala, M., 2009. Correction to "New parameterization of sulfuric acid-ammonia-water ternary nucleation rates at tropospheric conditions." J. Geophys. Res. 114, D09206. doi:10.1029/2009JD012136

Michel Flores, J., Bar-Or, R.Z., Bluvshtein, N., Abo-Riziq, a., Kostinski, a., Borrmann, S., Koren, I., Koren, I., Rudich, Y., 2012. Absorbing aerosols at high relative humidity: Linking hygroscopic growth to optical properties. Atmos. Chem. Phys. 12, 5511–5521. doi:10.5194/acp-12-5511-2012

Middlebrook, A., Bahreini, R., 2008. Applying Laboratory Collection Efficiencies to Ambient Field Data, AMS Users' Meeting, in: AMS Users' Meeting 2008.

Mohr, C., DeCarlo, P.F., Heringa, M.F., Chirico, R., Slowik, J.G., Richter, R., Reche, C., Alastuey, a., Querol, X., Seco, R., Peñuelas, J., Jiḿenez, J.L., Crippa, M., Zimmermann, R., Baltensperger, U., Prévôt, a. S.H., 2012. Identification and quantification of organic aerosol from cooking and other sources in Barcelona using aerosol mass spectrometer data. Atmos. Chem. Phys. 12, 1649–1665. doi:10.5194/acp-12-1649-2012

Morawska, L., Johnson, G., Ristovski, Z.D., Agranovski, V., 1999. Relation between particle mass and number for submicrometer airborne particles. Atmos. Environ. 33, 1983–1990. doi:10.1016/S1352-2310(98)00433-6

Neuman, J. a., 2003. Variability in ammonium nitrate formation and nitric acid depletion with altitude and location over California. J. Geophys. Res. 108.

doi:10.1029/2003JD003616

Ng, N.L., Canagaratna, M.R., Jimenez, J.L., Zhang, Q., Ulbrich, I.M., Worsnop, D.R., 2011. Real-time methods for estimating organic component mass concentrations from aerosol mass spectrometer data. Environ. Sci. Technol. 45, 910–916. doi:10.1021/es102951k

O'Dowd, C., Ceburnis, D., Ovadnevaite, J., Martucci, G., Bialek, J., Monahan, C., Berresheim, H., Vaishya, A., Grigas, T., Jennings, S.G., McVeigh, P., Varghese, S., Flanagan, R., Martin, D., Moran, E., Lambkin, K., Semmler, T., Perrino, C., McGrath, R., 2012. The Eyjafjallajökull ash plume - Part I: Physical, chemical and optical characteristics. Atmos. Environ. 48, 129–142. doi:10.1016/j.atmosenv.2011.07.004

O'Dowd, C., McFiggans, G., Creasey, D.J., Pirjola, L., Hoell, C., Smith, M.H., Allan, B.J., Plane, J.M.C., Heard, D.E., Lee, J.D., Pilling, M.J., Kulmala, M., 1999. On the photochemical production of new particles in the coastal boundary layer. Geophys. Res. Lett. 26, 1707. doi:10.1029/1999GL900335

Ovadnevaite, J., Ceburnis, D., Canagaratna, M., Berresheim, H., Bialek, J., Martucci, G., Worsnop, D.R., O'Dowd, C., 2012. On the effect of wind speed on submicron sea salt mass concentrations and source fluxes. J. Geophys. Res. Atmos. 117, 1–11. doi:10.1029/2011JD017379

Ovadnevaite, J., Ceburnis, D., Plauskaite-Sukiene, K., Modini, R., Dupuy, R., Rimselyte, I., Ramonet, M., Kvietkus, K., Ristovski, Z., Berresheim, H., O'Dowd, C.D., 2009. Volcanic sulphate and arctic dust plumes over the North Atlantic Ocean. Atmos. Environ. 43, 4968–4974. doi:10.1016/j.atmosenv.2009.07.007

Ovadnevaite, J., Kvietkus, K., Marsalka, A., 2006. 2002 summer fires in Lithuania: Impact on the Vilnius city air quality and the inhabitants health. Sci. Total Environ. 356, 11–21. doi:S0048-9697(05)00243-3 [pii]\n10.1016/j.scitotenv.2005.04.013 [doi]

Paatero, P., 1997. Least squares formulation of robust non-negative factor analysis. Chemom. Intell. Lab. Syst. 37, 23–35. doi:10.1016/S0169-7439(96)00044-5

Paatero, P., Tapper, U., 1994. Positive Matrix Factorization - A Nonnegative Factor Model with Optimal Utilization of Error Estimates of Data Values.

Environmetrics 5, 111–126. doi:10.1002/env.3170050203

Pope, C.A., Dockery, D.W., 2006. Health Effects of Fine Particulate Air Pollution: Lines that Connect. J. Air Waste Manage. Assoc. 56, 709–742. doi:10.1080/10473289.2006.10464485

Pun, B.K., Seigneur, C., 2007. Investigative modeling of new pathways for secondary organic aerosol formation. Atmos. Chem. Phys. 7, 2199–2216. doi:10.5194/acpd-7-203-2007

Quinn, P.K., Bates, T.S., Baum, E., Doubleday, N., Fiore, A.M., Flanner, M., Fridlind, A., Garrett, T.J., Koch, D., Menon, and S., 2008. Short-lived pollutants in the Arctic: their climate impact and possible mitigation strategies. Atmos. Chem. Phys. 8, 1723–1735.

Raes, F., Dingenen, R. Van, Elisabetta, V., Wilson, J., Putaud, J.P., Seinfeld, J.H., Adams, P., 2002. Chapter 18 Formation and cycling of aerosols in the global troposphere. Dev. Environ. Sci. 1, 519–563. doi:10.1016/S1474-8177(02)80021-3

Rimselyte, I., Ovadnevaite, J., Ceburnis, D., Kvietkus, K., Pesliakaite, E., 2007. Chemical composition and size distribution of fine aerosol particles on the east coast of the Baltic Sea. Lith. J. Phys. 47, 523–529.

Ristovski, Z.D., Suni, T., Kulmala, M., Boy, M., Meyer, N.K., Duplissy, J., Turnipseed, A., Morawska, L., Baltensperger, U., 2010. The role of sulphates and organic vapours in growth of newly formed particles in a eucalypt forest. Atmos. Chem. Phys. 10, 2919–2926. doi:10.5194/acp-10-2919-2010

Robinson, A.L., Donahue, N.M., Shrivastava, M.K., Weitkamp, E. a, Sage, A.M., Grieshop, A.P., Lane, T.E., Pierce, J.R., Pandis, S.N., 2007. Rethinking organic aerosols: semivolatile emissions and photochemical aging. Science 315, 1259–1262. doi:10.1126/science.1133061

Roholm, K., 1937. The fog disaster in the Meuse Valley, 1930: a fluorine intoxication. J. Ind. Hyg. Toxicol. 18, 126–137.

Schmid, O., Karg, E., Hagen, D.E., Whitefield, P.D., Ferron, G. a., 2007. On the effective density of non-spherical particles as derived from combined measurements of aerodynamic and mobility equivalent size. J. Aerosol Sci. 38, 431–443. doi:10.1016/j.jaerosci.2007.01.002

Seinfeld, J.H., Erdakos, G.B., Asher, W.E., Pankow, J.F., 2001. Modeling the

formation of secondary organic aerosol (SOA). 2. The predicted effects of relative humidity on aerosol formation in the alpha-pinene-, beta-pinene-, sabinene-, delta 3-carene-, and cyclohexene-ozone systems. Environ. Sci. Technol. 35, 1806–1817. doi:10.1021/es001765+

Seinfeld, J.H., Pandis, S.N., 2006. Atmospheric Chemistry and Physics: From Air Pollution to Climate Change, 2nd edition. Wiley, Chichester.

Seinfeld, J.H., Pandis, S.N., 1998. Atmospheric Chemistry and Physics: From Air Pollution to Climate Change, Atmospheric chemistry and physics from air pollution to climate change Publisher New York NY Wiley 1998 Physical description xxvii 1326 p A WileyInterscience Publication ISBN 0471178152.

Symonds, R.B., Rose, W.I., B., Luth, G.J.S., Gerlach, T.M., 1994. Volcanic-gas studies; methods, results, and applications. Rev. Mineral. Geochemistry 30, 1–66.

Skrabalova, L., Brus, D., Anttila, T., Zdimal, V., Lihavainen, H., 2014. Growth of sulphuric acid nanoparticles under wet and dry conditions. Atmos. Chem. Phys. 14, 6461–6475.

Slowik, J., Stainken, K., Davidovits, P., Williams, L.R., Jayne, J.T., Kolb, C.E., Worsnop, D., Rudich, Y., DeCarlo, P., Jimenez, J., 2004. Particle Morphology and Density Characterization by Combined Mobility and Aerodynamic Diameter Measurements. Part 2: Application to Combustion-Generated Soot Aerosols as a Function of Fuel Equivalence Ratio. Aerosol Sci. Technol. 38, 1206–1222. doi:10.1080/02786826.2004.10399462

Solomon, S., Qin, D., Manning, M., Chen, Z., Marquis, M., Averyt, K.B., Tignor, M., Miller, H.L., 2007. IPCC, 2007: Climate Change 2007: The Physical Science Basis. Contribution of Working Group I to the Fourth Assessment Report of the Intergovernmental Panel on Climate Change, D Qin M Manning Z Chen M Marquis K Averyt M Tignor and HL Miller New York Cambridge University Press pp.

Solomon, S., D., Qin, M., Manning, Z., Chen, M., Marquis, K.B., Averyt, M.T., Miller HL, Solomon, S., Qin, D., Manning, M., Chen, Z., Marquis, M., Averyt, K.B., Tignor, M., Miller, H.L., 2007. Summary for Policymakers. In: Climate Change 2007: The Physical Science Basis. Contribution of Working Group I to the Fourth Assessment Report of the

Intergovernmental Panel on Climate Change. D Qin M Manning Z Chen M Marquis K Averyt M Tignor HL Mill. New York Cambridge Univ. Press pp Geneva, 996. doi:10.1038/446727a

Spencer, M.T., Shields, L.G., Prather, K. a., 2007. Simultaneous measurement of the effective density and chemical composition of ambient aerosol particles. Environ. Sci. Technol. 41, 1303–1309. doi:10.1021/es061425+

Straif, K., Cohen, A., Samet, J., 2013. IARC Scientific Publication No. 161 Air Pollution and Cancer.

Trenberth, K.E., Fasullo, J.T., Kiehl, J., 2009. Earth's global energy budget. Bull. Am. Meteorol. Soc. 90, 311–323. doi:10.1175/2008BAMS2634.1

Turpin, B.J., Lim, H.-J., 2001. Species Contributions to PM2.5 Mass Concentrations: Revisiting Common Assumptions for Estimating Organic Mass. Aerosol Sci. Technol. 35, 602–610. doi:10.1080/02786820152051454

Ulbrich, I.M., Canagaratna, M.R., Zhang, Q., Worsnop, D.R., Jimenez, J.L., 2009. Interpretation of Organic Components from Positive Matrix Factorization of Aerosol Mass Spectrometric Data. Atmos. Chem. Phys. 9, 2891. doi:10.5194/acp-9-2891-2009

von Glasow, R., Bobrowski, N., Kern, C., 2009. The effects of volcanic eruptions on atmospheric chemistry. Chem. Geol. 263, 131–142. doi:10.1016/j.chemgeo.2008.08.020

Whitby K.T., Cantrell B.K., 1976. Proceedings of the International Conference on Environmental Sensing and Assessment (ICESA), Institute of Electrical and Electronic Engineers (IEEE) 1976. Atmospheric aerosols: characteristics and measurement., in: ICESA Paper 29-1. p. IEEE. p. 6.

Williams, J., de Reus, M., Krejci, R., Fischer, H., Ström, J., 2002. Application of the variability-size relationship to atmospheric aerosol studies: estimating aerosol lifetimes and ages. Atmos. Chem. Phys. Discuss. 2, 43–74. doi:10.5194/acpd-2-43-2002

Xing, L., Fu, T.M., Cao, J.J., Lee, S.C., Wang, G.H., Ho, K.F., Cheng, M.C., You, C.F., Wang, T.J., 2013. Seasonal and spatial variability of the OM/OC mass ratios and high regional correlation between oxalic acid and zinc in Chinese urban organic aerosols. Atmos. Chem. Phys 13, 4307–4318.

Xu, L., Penner, J.E., 2012. Global simulations of nitrate and ammonium aerosols and their radiative effects. Atmos. Chem. Phys. 12, 9479–9504. doi:10.5194/acp-12-9479-2012

Zaveri, R. a., Shaw, W.J., Cziczo, D.J., Schmid, B., Ferrare, R. a., Alexander, M.L., Alexandrov, M., Alvarez, R.J., Arnott, W.P., Atkinson, D.B., Baidar, S., Banta, R.M., Barnard, J.C., Beranek, J., Berg, L.K., Brechtel, F., Brewer, W. a., Cahill, J.F., Cairns, B., Cappa, C.D., Chand, D., China, S., Comstock, J.M., Dubey, M.K., Easter, R.C., Erickson, M.H., Fast, J.D., Floerchinger, C., Flowers, B. a., Fortner, E., Gaffney, J.S., Gilles, M.K., Gorkowski, K., Gustafson, W.I., Gyawali, M., Hair, J., Hardesty, R.M., Harworth, J.W., Herndon, S., Hiranuma, N., Hostetler, C., Hubbe, J.M., Jayne, J.T., Jeong, H., Jobson, B.T., Kassianov, E.I., Kleinman, L.I., Kluzek, C., Knighton, B., Kolesar, K.R., Kuang, C., Kubátová, a., Langford, a. O., Laskin, a., Laulainen, N., Marchbanks, R.D., Mazzoleni, C., Mei, F., Moffet, R.C., Nelson, D., Obland, M.D., Oetjen, H., Onasch, T.B., Ortega, I., Ottaviani, M., Pekour, M., Prather, K. a., Radney, J.G., Rogers, R.R., Sandberg, S.P., Sedlacek, a., Senff, C.J., Senum, G., Setyan, a., Shilling, J.E., Shrivastava, M., Song, C., Springston, S.R., Subramanian, R., Suski, K., Tomlinson, J., Volkamer, R., Wallace, H.W., Wang, J., Weickmann, a. M., Worsnop, D.R., Yu, X.Y., Zelenyuk, a., Zhang, Q., 2012. Overview of the 2010 Carbonaceous Aerosols and Radiative Effects Study (CARES). Atmos. Chem. Phys. 12, 7647–7687. doi:10.5194/acp-12-7647-2012

Zhang, Q., Canagaratna, M.R., Jayne, J.T., Worsnop, D.R., Jimenez, J.L., 2005. Time- and size-resolved chemical composition of submicron particles in Pittsburgh: Implications for aerosol sources and processes. J. Geophys. Res. Atmos. 110, 1–19. doi:10.1029/2004JD004649

Zhang, Q., Jimenez, J.L., Canagaratna, M.R., Allan, J.D., Coe, H., Ulbrich, I., Alfarra, M.R., Takami, a., Middlebrook, a. M., Sun, Y.L., Dzepina, K., Dunlea, E., Docherty, K., DeCarlo, P.F., Salcedo, D., Onasch, T., Jayne, J.T., Miyoshi, T., Shimono, a., Hatakeyama, S., Takegawa, N., Kondo, Y., Schneider, J., Drewnick, F., Borrmann, S., Weimer, S., Demerjian, K., Williams, P., Bower, K., Bahreini, R., Cottrell, L., Griffin, R.J., Rautiainen, J., Sun, J.Y., Zhang, Y.M., Worsnop, D.R., 2007. Ubiquity and dominance of oxygenated species in organic aerosols in anthropogenically-influenced Northern Hemisphere midlatitudes.

Geophys. Res. Lett. 34, 1–6. doi:10.1029/2007GL029979

Zhang, Q., Jimenez, J.L., Canagaratna, M.R., Ulbrich, I.M., Ng, N.L., Worsnop, D.R., Sun, Y., 2011. Understanding atmospheric organic aerosols via factor analysis of aerosol mass spectrometry: A review. Anal. Bioanal. Chem. 401, 3045–3067. doi:10.1007/s00216-011-5355-y